



HHS Public Access

Author manuscript

Adv Healthc Mater. Author manuscript; available in PMC 2018 January 01.

Published in final edited form as:

Adv Healthc Mater. 2017 January ; 6(1): . doi:10.1002/adhm.201601118.

3D Bioprinting for Organ Regeneration

Dr. Haitao Cui,

Department of Mechanical and Aerospace Engineering, The George Washington University, 3590 Science and Engineering Hall, 800 22nd Street NW, Washington, DC 20052, USA

Margaret Nowicki,

Department of Biomedical Engineering, The George Washington University, 3590 Science and Engineering Hall, 800 22nd Street NW, Washington, DC 20052, USA

Prof. John P. Fisher, and

Department of Bioengineering University of Maryland 3238 Jeong H. Kim Engineering Building College Park, MD 20742, USA

Prof. Lijie Grace Zhang*

Department of Medicine, The George Washington University, 3590 Science and Engineering Hall, 800 22nd Street NW, Washington, DC 20052, USA

Abstract

Regenerative medicine holds the promise of engineering functional tissues or organs to heal or replace abnormal and necrotic tissues/organs, offering hope for filling the gap between organ shortage and transplantation needs. Three-dimensional (3D) bioprinting is evolving into an unparalleled bio-manufacturing technology due to its high-integration potential for patient-specific designs, precise and rapid manufacturing capabilities with high resolution, and unprecedented versatility. It enables precise control over multiple compositions, spatial distributions, and architectural accuracy/complexity, therefore achieving effective recapitulation of microstructure, architecture, mechanical properties, and biological functions of target tissues and organs. Here we provide an overview of recent advances in 3D bioprinting technology, as well as design concepts of bioinks suitable for the bioprinting process. We focus on the applications of this technology for engineering living organs, focusing more specifically on vasculature, neural networks, the heart and liver. We conclude with current challenges and the technical perspective for further development of 3D organ bioprinting.

1. Introduction

Human organs are highly complex structures formed by the combined, functional organization of multiple tissue types. The cells in these organs are highly specialized and group together to perform distinctive functions.^[1] Organ dysfunction or failure is drastically increasing due to traumatic injury and disease.^[2] Often, clinical treatments are limited by a paucity of available donors and immune rejection of donated tissue.^[3] In the search for alternatives to conventional treatment strategies for the repair or replacement of missing or

*L. G. Zhang, lgzhang@gwu.edu.

malfunctioning human tissues and organs, tissue engineering approaches are being explored as a promising solution.^[2–4]

Presently, tissue engineering approaches have been widely studied in cartilage, bone, skin, vascular tissue and nerve regeneration, among others.^[4–7] When designing a tissue engineered scaffold, the combination of material, biological and engineering requirements must be considered in an application-specific manner.^[8–11] Biomimetic design of the scaffolds, including 3D structural characteristics and physical properties, can substantially enhance the physiological performance through appropriate cell–cell and cell–matrix interactions, further enhancing biological functions.^[10,12,13] However, most 3D scaffolds currently fabricated with traditional techniques lack these qualities.^[14] Although significant successes have been achieved in engineered tissues, both in research and clinical applications, it is obvious that complex 3D organs require more precise multicellular structures with vascular and neural network integration. These requirements cannot be fulfilled using traditional methods.^[15–17]

3D printing is a rapid prototyping and additive manufacturing technique used to fabricate complex architecture with high precision through a layer-by-layer building process.^[18] This automated, additive process facilitates the manufacturing of 3D products having precisely controlled architecture (external shape, internal pore geometry, and interconnectivity) with highly reproducibility and repeatability.^[9,19] Therefore, in the regeneration field, it can provide an excellent alternative for biomimetic scaffold fabrication by accurately positioning multiple cell types and biofactors simultaneously into complex multi-scale architectures that better represent the structural and biochemical complexity of living tissues or organs.^[18,20,21] In the past three decades, 3D bioprinting has been widely developed to directly or indirectly fabricate 3D cell scaffolds or medical implants for the field of regenerative medicine. It offers very precise spatiotemporal control on placement of cells, proteins, DNA, drugs, growth factors, and other bioactive substances to better guide tissue formation for patient-specific therapy.^[20,22,23] 3D printing of bioactive scaffolds contains two types of scaffold fabrication: acellular functional scaffolds which incorporate biological components, and cell-laden constructs aiming to replicate native analogues.^[21,24] Both of them aim to produce biocompatible, implantable constructs for tissue/organ regeneration, thus we refer to 3D printing in the context of bioactive scaffold fabrication as “bioprinting”. In this regard, the term bioprinting does not indicate whether cells are directly printed or involved at any stage of the fabrication process.

An essential requirement for reproducing the complex, heterogeneous architecture of functional tissues or organs is a comprehensive understanding of the composition and organization of their components.^[10,11] Therefore, medical imaging technology is an indispensable tool to provide information on 3D structure and function at the cellular, tissue, organ and organism levels, aiding the design of a patient-specific construct.^[20,25] It commonly offers noninvasive imaging modality, including computed tomography (CT) and magnetic resonance imaging (MRI). Computer-aided design (CAD) and computer-aided manufacturing (CAM) tools and mathematical modeling are also used to collect and digitize the complex tomographic and architectural information for tissues.^[25] The 3D imaged tissue or organ model is divided into 2D horizontal slices that are imported into a 3D bioprinter

system for the layer-by-layer deposition. Considering the available 3D bioprinting techniques, the cell types (differentiated or undifferentiated), biomaterials (synthetic or natural), and supporting biochemical factors are then selected, and the configuration of these printing components drives the construction of the 3D tissues and organs. This integrated technique (imaging-design-fabrication) can recreate more complex 3D organ level structures and incorporate mechanical as well as biochemical cues that are crucial elements of the whole organ architecture.^[20,26] In addition, this technique has the capacity to build a 3D tissue-or organ-specific microenvironment by mimicking the natural, highly dynamic yet variable 3D structures, mechanical properties, and biochemical microenvironments.^[27] In this manner, 3D bioprinting for organ regeneration involves additional strategies for printing multiple living cells, including vasculature and neural network integration, and eventually developing the specific functions of 3D bioprinted organ analogues.

Charles W. Hull, in 1986 received a patent for the liquid, photopolymer-based manufacturing technology of stereolithography; this proved to be the pioneering work for future 3D printing techniques.^[28] In 2003, a cellular bioprinting technique based on traditional 2D inkjet technology was proposed.^[29] In 2009, Organovo and Invetech created one of the first commercial 3D bioprinters.^[30,31] Finally in 2016, the Food and Drug Administration (FDA) issued draft guidance, titled “Technical Considerations for Additive Manufactured Devices”, which provided guidance for 3D printing techniques and products.^[32] Currently, with the increasing global interest and need, more and more businesses have been established in the expanding bioprinting market, such as 3D Systems (Rock Hill, SC, USA), Hewlett-Packard (Palo Alto, CA, USA), Novogen MMX Bio-printer (Organovo, Inc., San Diego, CA, USA), 3D Bioplotter (EnvisionTEC, Gladbeck, Germany), Oxford Performance Materials (South Windsor, CT, USA), and Commercial Blood Vessel Bioprinter (Revotek, Sichuan, China) among others.^[31] By 2022, the global 3D bioprinting market is expected to reach \$1.82 billion and will include products and materials for dental, medical, analytical, and food applications.^[31] Although still in its infancy considering the complexity and functionality, this technology appears to show great promise for advancing tissue engineering toward organ fabrication, ultimately mitigating organ shortage and saving lives.

In this review, we focus on general principles, techniques, and other essential elements pertaining to the application of 3D bioprinting technologies for generating 3D tissues and organs. We propose a stepwise process of regenerating a complex tissue/organ, and also present recent advances in 3D bio-printing for organ regeneration. Furthermore, we discuss current challenges and exciting opportunities of 3D bioprinting technologies toward creating realistic organs that further fundamental research and translational medicine (Figure 1).

2. 3D Tissue/Organ Bioprinting and Related Manufacturing Strategies

2.1. Fundamental Principles

3D bioprinting is basically a rapid prototyping and additive manufacturing technique used to fabricate artificial implants or complex tissue constructs through a layer-by-layer building process for patient-specific therapy. 3D bioprinting shares three basic concepts with ordinary 2D printing – desktop printer (3D printer), print file (3D model file), ink (bioink consisting of biomaterials, bioactive components and cells), and paper (print platform). Unlike 2D

printing, 3D bioprinting is a comprehensive process requiring various design considerations, including imaging, modeling, printer choice, bioink selection, culture condition, and 3D construct development among others. Generally, the manufacturing activities can be divided into three steps: pre-bioprinting (modeling), bioprinting, and post-bioprinting.

Pre-bioprinting, also known as modeling, mainly includes 3D imaging acquisition, digital 3D design and bioink/biomaterial selection based on the type of 3D bioprinting model.^[20] Several imaging technologies, such as 3D scanner, CT, MRI and others, are applied to collect and digitize the complex tomographic and architectural information of tissues. Giesel et al. described and discussed the various methods of 3D imaging technology for 3D printing applications in detail.^[25] The desired structure of digital 3D models is precisely created using CAD software and stored as a stereolithography (stl) files. Bioink or biomaterial selection depends on the specific bioprinter type and the product properties required.

The 3D structure with patient-specific design is then printed in layer-by-layer deposition modeling process in the bio-printing phase. According to the program design of different printers, the 3D design files can be directly loaded into the printer, or must first be passed through a slicing program for further modification before being imported into the printer. The slicing program can parse the solid object into a stack of thin, axial cross sections; each respective 2D cross section is reproduced integrating various infill patterns, as programmed. In this step, the printer reads the stl file and deposits successive layers of liquid, powder, or several other materials to build the 3D model from a series of 2D cross-sections. Several 3D printing techniques are capable of using multiple nozzles (multiple materials), adjustable angles, and even multiple printing combinations.

3D bioprinting for tissue engineering applications can be divided into two forms, with and without incorporated living cells printed directly into the constructs. Cellular bioprinting techniques can directly deposit bioinks with viable cells to form a 3D living structure. Based on the working strategies, they can primarily be classified into three categories, droplet-based, extrusion-based and laser-assisted bioprinting.^[20,33] Variations in the available bioprinting technologies also affect the characteristics of living tissue/organ constructs. Comparatively, acellular bioprinting techniques provide more extensive choices for tissue regeneration applications.^[18] Without the consideration of cell viability or bioactive components, several 3D printing techniques with higher temperatures, chemicals and other harsh environments can be utilized to manufacture implants.^[34] Considering the specific requirements of the targeted tissues/organs properties, the design must take into account the capabilities and properties of the bioprinting systems (both bioinks and bioprinters), which we discuss next in detail.

Finally, post-bioprinting, which involves the development of biomimetic structures, mechanical supports and biological functionality, is an essential step to develop mature tissues/organs for living applications.^[35,36] Several additional manufacturing techniques, including substrate supports and sacrificial templates, among others, are potentially required to create higher mechanical elasticity/strengths, more precise structures, more complex structures or multiple biological functions due to current printing technique limitation.^[16] More importantly, in vitro culture (preference in a bioreactor), in vivo implantation, or even

in situ bioprinting will be performed to induce and enhance construct maturation thereby transforming constructs into functional tissues/organs.^[26] Figure 2 shows a tree-diagram of the various 3D bioprinting techniques with simplified illustrations of typical 3D bioprinting techniques.

2.2. Accustomed Bioprinting Techniques

Typically, ASTM (F2792) standard terminology for 3D printing technologies consists of several parts including vat photopolymerization, material jetting, material extrusion, powder bed fusion, binder jetting, sheet lamination, and directed energy deposition.^[37] To some extent, the terminology of bioprinting techniques more specifically refers to both the bioink formulations and printing modality. Acellular bioprinting is divided into two forms, direct implantation and cell post-seeding. The acellular implant serves as a nonliving implant device or artificial graft substitute, while the cellular implant often requires an extra step depositing cells onto the constructs after acellular bioprinting. In contrast, the direct cellular bioprinting is a one-step process of generating a rapid prototyped tissue by accomplishing both the construct fabrication and cellularization jointly.

2.2.1. Cellular Bioprinting—Cellular 3D bioprinting directly employs living cells in the construct fabrication process together with the inherent advantages of 3D printing-based rapid prototyping. Diverse techniques have been developed to create 3D living tissue/organ analogues, and each of them has different features (strengths and limitations) in terms of the available conditions such as biological materials, resolution, printing speed and cell viability. Depending on the printing modality (bioink deposition mechanism), the representative techniques of cellular bioprinting can be categorized into three types: droplet-based, extrusion-based, and stereolithography.^[14,20,22,38]

Droplet-based bioprinting relies on various energy sources (thermal-, electric-, laser beam-, acoustic- or pneumatic- mechanisms) to pattern the bioink micro-droplets of living cells and other biologicals in a high-throughput manner. It offers greater advantages due to its simplicity and agility with precise control on deposition of biologicals including cells, growth factors, and genes for tissue/organ regeneration. It has also been the most common for pharmaceutical use due to its simplicity, versatility, and high-throughput capability.

Extrusion-based (dispensing, or direct writing) bioprinting which originates from fused deposition modeling (FDM) printing uses pneumatic-, mechanical- or electromagnetic-driven systems to deposit cells based on a “needle-syringe” type. During bioprinting, bioink dispensed by a deposition system precisely prints cell-laden filaments forming desired 3D structures.

Stereolithography-based (vat-photopolymerization) bioprinting mainly utilizes laser energy to deposit cell-laden bioink in a reservoir via beam scanning or image projection modeling, allowing the molding of the high-precision patterns. It offers greater advantages due to the precise control on deposition of biologicals and high resolution.

2.2.1.1. Droplet-Based Cellular Bioprinting (DCB): The key feature of droplet-based bioprinting is that the droplets of cell-laden bioink (hydrogels or slurries) are generated and

deposited to pre-defined locations on the substrate. As a noncontact bio-printing technique, it provides a high-throughput method for depositing multiple cells or biologicals in small droplets onto a targeted spatial position. Droplet techniques can be classified into four categories: inkjet, electrohydrodynamic jetting, pneumatic pressure assisted-, and laser assisted- droplet bioprinting.^[39–42]

The inkjet bioprinting, which is granted with the earliest cellular printing patent, is originated from commercial 2D inkjet printing.^[29] The necessary equipment is easily remolded from 2D inkjet desktop printers making this technology widely available and relatively inexpensive. In this technique, the bioink solution including biomaterial, bioactive factors, and cells is stored in a cartridge or reservoir, and then transferred to the ink chamber for droplet ejection. The droplets can be generated by two mechanisms, thermal or piezoelectric actuation, which can be ejected from the inkjet-head nozzle to the print surface.^[43] They operate similar to the traditional “drop-on-demand” 2D inkjet printers. The thermal actuation is based on a heating element, which can superheat the bioink to create vapor bubbles for ejecting the droplets. Although the temperature reaches 200~300 °C, the process only persists for a few microseconds (~2 μs) resulting in an overall temperature rise of ~10 °C in the printer head. Many results have demonstrated that this increase in temperature causes minimal damage to the viability of both printed cells and other integrated biologicals. The piezoelectric technique employs a voltage to induce a rapid shape change of the piezoelectric material, which generates a pressure pulse in the fluid forcing a droplet of ink from the nozzle. Droplet shape and size can be adjusted by tuning the applied voltage to the piezoelectric material. It allows a wider variety of inks than thermal inkjets as there is no requirement for a volatile component, and no issue with coagulation. The acoustic radiation force associated with the ultrasound field is also utilized to eject the droplets from an air-liquid interface on the piezoelectric printer.^[44] Ultrasound parameters, including pulse, duration and amplitude, can be adjusted to control the size of droplets and the rate of ejection. The acoustic radiation is capable of generating and controlling uniform droplet size and ejection directionality. However, the acoustic frequencies used in these printers have the potential to induce damage of the cell membrane and cell lysis. Additionally, several modified inkjet techniques with multi-jets have been developed to build complex tissue and organ prototypes by arranging multiple cell types and other tissue components.^[45] Overall, the inkjet bioprinting technique ensures rapid fabrication with highly repeatable patterns; additionally, small volume droplets enable high printing resolution (lower to 50 μm). Moreover, inkjet bioprinting typically exhibits over 80% cell viability after cellular bioprinting.^[20] Inkjet bioprinters do, however, still have limitations on material viscosity, cell density and mechanical strength. Devices are typically compatible with low solution viscosities (below 0.01 Pa•s) and low cell concentrations (fewer than 10 million cells/mL), avoiding high shear stress and nozzle clogging.^[20]

The electrohydrodynamic jetting (electrospraying or electrospinning) applies an electric potential difference between a positively charged needle and a grounded electrode to generate repulsive Coulombic force. Droplet ejection occurs, in the micrometer to nanometer size range, when the charged medium exiting the needle enters the high-intensity electric field.^[39,46,47] The size and distribution of these droplets can be controlled through the applied potential difference, the flow rate to the needle, the distance of electrodes and the

liquid solution properties.^[48] Inkjet bioprinting dimensions are currently limited by the diameter of the jetting needle. Typically, droplet diameter is approximately two times the size of the needle diameter; as such, this technology has limitations in the size range of tens of nanometers. In contrast to inkjet technology, electrohydrodynamic jetting does not suffer from these limitations and can be used to process concentrated suspensions from needles that are a few hundred micrometers in size yet are capable of generating droplet deposits a few micrometers in size and smaller. Furthermore, no adverse effects on cell viability have been observed when jetting the cell-laden bioinks.^[49]

The pneumatic pressure technique uses a set of electromechanical micro-valves where the droplets are produced by opening the micro-valve under constant pneumatic pressure.^[42] This technique uses various types of liquid biomaterials with viscosities of up to 200 Pa•s, and controls the droplet volume by adjusting the pressure to the fluidic pathway and valve gating time. Although a higher liquid viscosity can be applied, there remain several concerns regarding droplet controls and cell viability. In order to obtain a favorable printing structure, the effect of the printing conditions must be fully considered to include substrate stiffness, material preparation, droplet size, printing speed, surfactant usage, and agitation among others.^[22]

However, for the inkjet and pneumatic pressure assisted bioprinting, the viscosity of the available bioinks is too low to facilitate the rapid generation and sustainment of 3D structures. Therefore, additional cross-linking methods are applied to address this limitation, including UV/Vis light, pH, temperature or chemical reagents. The photocurable materials can be independently used, associated as the droplet bioinks, or deposited as supporting materials to assist in 3D molding. Additionally, multi-jet bioprinting strategies can be used to co-print the bioinks and the cross-linkers in turn, allowing the generation of a solid, stable 3D structure. The crosslinking procedure may slow down the printing process, and several crosslinking methods may result in excessive damage of cell viability and biological functionality; these risks must be considered and managed carefully during fabrication.

In addition to the high resolution, simple processing, and low cost benefits of these bioprinting techniques, another advantage is the potential to introduce concentration gradients of cells, materials or growth factors throughout the 3D structure by altering droplet densities or sizes. Recent developments of this technique have reported controlling droplet sizes and deposition rates ranging from 1 pL to 300 pL in volume with up to 10 000 droplets/s. Droplet bioprinting also shows great promise for “scaffold-free” bioprinting by depositing layers of cells into a sacrificial mold.

Besides the three aforementioned droplet techniques, laser-assisted droplet systems have also been developed.^[40] Differing from several other reviews that listed it as a laser-assisted bio-printing technique individually, we combine it into droplet bioprinting because of some similarities. Laser-assisted droplet bioprinting (also known as laser-induced forward transfer or LIFT), consists of a pulsed laser source, a donor layer (this includes a laser-energy-absorbing layer, such as gold or titanium, and a bioink layer) and a receiving substrate. It utilizes a focused laser to pulse on the absorbing layer generating a high-pressure bubble that propels cell-laden droplets onto the substrate. The absorbing layer is used to transfer heat for

bioink droplet production; this prevents from direct laser. The droplet volume can be controlled from 10 to 7000 pL by adjusting the viscosity and thickness of the bioink layer contributing to a higher printing resolution. The resolution is also influenced by many additional factors, including the laser fluence, the surface tension, the wettability of the substrate, the air gap between the donor layer and the substrate, and the thickness and viscosity of the bioink layer. Moreover, this technique is capable of employing a high cell densities (up to 10^8 cells/mL) and as well as high bioink viscosity (1~300 mPa•s) because of its nozzle-free droplet model. Despite these advantages, a relatively low efficiency, high cost and limited availability of bioinks for this technique are still major concerns.

2.2.1.2. Extrusion-Based Cellular Bioprinting (ECB): Extrusion-based (or dispensing, direct writing) bioprinting is an integrated technique consisting of a fluid-dispensing system for extrusion control and an automated robotic system for bioprinting.^[20,22] The bioink is extruded into the manner of cell-laden cylindrical filaments or discrete volumes of bioinks that can be precisely deposited into the desired 3D structures. Continuous deposition provides better structural integrity during rapid fabrication. Dispensing systems can be classified into three types: pneumatic-, mechanical- (piston or screw), and solenoid-based microextrusion.^[50]

Pneumatic-based systems utilize pressurized air to extrude filaments using a valve-free or a valve-based configuration. Compared to the valve-free configuration, the valve-based configuration possesses a higher precision due to a controlled pressure and pulse frequency.^[42] Mechanical micro-extrusion (or direct writing) provides a simpler and more direct method of controlling the bioink printing.^[51–53] The piston system commonly composed of syringes and needles is suitable to a fluid with low viscosity, whereas the screw system is capable of generating a larger pressure for dispensing the bioinks with higher viscosities.^[50] However, a large shearing force along the nozzle in mechanical micro-extrusion can potentially harm the laden cells. Solenoid (or electromagnetic driven) microextrusion applies electrical pulses to open a valve by canceling the magnetic pull force generated between a floating ferro-magnetic plunger and a ferro-magnetic ring magnet.^[42] Mechanical dispensing systems might provide more direct control over the material flow, because of the delay of the compressed gas volume in pneumatic systems and the high complexity of electromagnetic driven systems. Materials with viscosities ranging from 30 to $>6 \times 10^7$ mPa•s have been shown to be compatible with microextrusion bioprinters, with higher-viscosity materials often providing structural support for the printed construct and lower-viscosity materials providing a suitable environment for maintaining cell viability and function.^[52]

In addition to dispensing systems, the extrusion printers include a stage and one or more cartridges (i.e., syringes or pens) that can be loaded with cell-laden bioinks or other biologicals for printing. The materials inside the cartridges may be dispensed using a microextrusion system. The printing process can be controlled by the dispensing procedure, speed, nozzle size, the displacement of the cartridge, and/or the stage motion in x , y , and z axes. Moreover, several advanced techniques have been developed for the cartridges and the stages such as: temperature-controlled cartridge (nozzle) or stage systems, multiple

independently controlled nozzles or chambers, multiple direction-controlled nozzle or stage systems, and coaxial nozzle systems, among others.^[20,50,54]

Compared to droplet-based bioprinting, extrusion-based bio-printing enables rapid printing, easy operation and a wide selection of bioinks, including cell aggregates, cell-laden hydrogels, micro-carriers, decellularized matrices and synthetic polymer fibers. Synthetic polymers that have relatively high mechanical strength are often employed to reinforce printed 3D tissue/organ analogues. There are two main types of bioinks used in microextrusion systems.^[50] The first is high-viscosity, cell-laden solutions or low-modulus cell-laden hydrogels, which need be rapidly solidified into a 3D construct after extrusion. However, the printing conditions of the cell-laden hydrogel are somewhat limited by high shear force management. Another type involves using spherical and cylindrical multicellular systems with or without supportive biomaterials as a bioink; cell spheroids and cell-laden microcarriers are two examples of this type of bioink. After printing, the multicellular systems fuse together to replicate the 3D tissue structure. This technique directly prints solid cellular units enabling scaffold-free bioprinting, or printing free of exogenous biomaterials. In order to obtain appropriate mechanical integrity of a 3D configuration, the molding process and the properties of bioinks, as well as their interactions, are very important considerations for extrusion printing and must be addressed in the experimental design.^[50] The typical molding processes include: (1) self-assembly (i.e., shear-thinning materials, self-healing materials), (2) crosslinking agent integration (i.e., pre-crosslinked bioink, bioplotting, coaxial crosslinking, aerosol crosslinking or spraying crosslinking system), (3) UV/Vis photocuring and (4) environmentally sensitive deposition (pH, temperature, and others). In extrusion based bioprinting, bioplotting refers to syringe dispensing system requiring a curing process involving additional solidification over time.^[50,55] Therefore, we do not separately introduce it as a bioprinting technique. In the bioplotting approach, cell-laden bioinks are directly extruded into a plotting medium (crosslinking pool) to complete the curing process. It requires the use of relatively viscous bioinks printed into plotting medium that can support the extruded structures temporarily until crosslinking is complete.^[56]

Overall, extrusion-based techniques are capable of greater deposition and printing speed and have more tolerance for heterogeneous formulations, allowing physiologically relevant cell densities, which facilitate scalability in a relatively short period of time. Despite its versatility and great benefits, extrusion-based bioprinting still has several challenges mainly involving lower resolutions, higher shear stresses, and limited material selection among others. The minimum feature size of the technology is generally over 100 μm ; nonbiological microextrusion printers are capable of 5 μm resolution.^[20,50] Bioinks should possess shear thinning ability to overcome surface tension to extrude in filament form. The resulting high shear stress at the nozzle may decrease the cell viability. Cell viability after microextrusion bioprinting is typically lower than that with inkjet-based bio-printing; cell survival rates are in the range of 40~86%, controllable by changing extrusion speed and nozzle gauge.^[50]

2.2.1.3. Stereolithography-Based Cellular Bioprinting (SCB): Stereolithography appearance (SLA) offers an additive manufacturing technique with very high resolution and accuracy.^[20,22,57] The Stereolithography-based bioprinting technique (vat

photopolymerization) utilizes the spatially controlled irradiation of light or laser to solidify a geometrically 2D pattern layered through selective photopolymerization in the bioink reservoir. The 3D structure can be consecutively built on 2D patterned layers in a “layer-by-layer” fashion, and the uncured bioink can be easily removed from the final product. The photo-polymerization of 2D patterned layers is the most crucial step in SLA-based bioprinting. Traditional SLA-based bioprinting techniques have two types: beaming-scanning and mask-image-projection.^[22,24,58]

The beam-scanning technique, or laser direct writing (LDW), uses a laser beam to scan photocurable bioinks for solidification of a 2D patterned layer.^[59] The resolution is dependent on irradiant exposure conditions (laser spot size, wavelength, power, exposure time/velocity and the occurrence of absorption or scattering of the laser beam), and the selection of photo-initiator or any UV absorbers.^[60,61] The types and concentration of bioinks, scanning speed and laser power contribute to the overall mechanical properties of the bioprinted structure. Additionally, when printing multiple layers, early layers may be repeatedly exposed to the laser, causing uneven mechanical strength or undesired 3D structures/patterns. With the development of micro-stereolithography (μ SLA) techniques, a resolution of about 5 μ m in the x/y plane and 10 μ m in the z axis can be achieved.^[62,63]

The mask-image-projection printing system dynamically generates a defined mask image that is projected onto the surface of the photocurable bioinks using a digital light procession technique (DLP), which can solidify an entire 2D patterned layer simultaneously.^[22,37,57,58] The DLP system uses a digital micromirror device (DMD) to project a set of 2D images from the horizontally sliced 3D structure. Compared to the beam-scanning technique, mask-image-projection printing can be much faster due to its ability to simultaneously form the shape of an entire layer.

There is a limited choice of photopolymerizable bioinks, however polymer modification can technically enable more options.^[58] The commonly photocurable bioinks include polyethylene glycol acrylate/methacrylate and its derivatives, methacrylated/acrylated natural biomaterials (gelatin, hyaluronic acid, dextran, and others), and methacrylated/acrylated capped among other synthetic polymers. Overall, the main advantages of stereolithography-based bioprinting techniques are their ability to simply fabricate complex designs with high resolution and rapidly print constructs without support material. Most commercial systems prepare structures with low to 50 μ m features; μ SLA systems are capable of preparing structures with <5 μ m features.^[57] However, the photopolymerization is driven by a radically induced chemical reaction, and the free radicals can damage the cell membrane, proteins, and nucleic acids. This technique can achieve up to 40~80% cell viability depending on the laser wavelength, power, exposure time and toxicity of photo-initiator.^[22,57] Therefore, it is important to apply a cytocompatible photo-initiator. Additionally, the limited availability of photocurable biomaterials and high equipment costs are major concerns with this technology.

2.2.2. Acellular Bioprinting—Compared to cellular bioprinting techniques, acellular 3D bio-printing provides more extensive choices for material selection and manufacturing method. The aforementioned cellular bio-printing techniques can also employ acellular

bioinks to fabricate tissue engineered scaffolds. An additional cell seeding technique can be employed to create artificial 3D cell-laden scaffolds for tissue/organ regeneration after printing. Here, a universal cell seeding procedure can be used in a post-seeding process, or perfusable cell seeding can be obtained using a bioreactor device. Also 3D printed grafts without cells can be directly implanted into injured patients for functional replacement or structural support during healing. The representative techniques of acellular bioprinting fall into two categories: extrusions-based acellular bioprinting (EAB) or laser-based acellular bioprinting (LAB).

2.2.2.1. Extrusion-Based Acellular Bioprinting (EAB): Unlike the previously presented extrusion systems focusing on cellular bioprinting, acellular extrusion (or acellular direct writing) can utilize volatile or easily displaced organic solvents to dissolve polymers, followed by conversion from a highly viscous solution to solid 3D structures.^[51,64] After removing the organic solvent thoroughly, the cells can be seeded and grown on the scaffold's surface for tissue/organ regeneration.

Fused deposition modeling (FDM) or fused filament fabrication (FFF) was developed in the early 1990s and is a major acellular, extrusion-based system.^[18,21,34,37] It is the most widely used and generally well-explored 3D printing strategy because it is low-cost and relatively fast. This technique employs thermoplastic filaments that are heated to their melting point or to a semimolten state, passed through an extrusion nozzle and allowed it to solidify on the printing stage without any additional crosslinking requirement.^[18,65] This method is analogous to conventional extrusion or injection molding except molds are not used. Multiple print heads can be accommodated to permit co-printing of temporary support material for complex overhanging structures or multiple material integration with different properties within a single structure for complicated construct fabrication. The printer is composed of heating blocks with temperature controllers, an extrusion block and motors.^[58] The extrusion force is driven pneumatically or mechanically with a lead screw. These models result in an overall resolution of $>50\ \mu\text{m}$ in layer height and an accuracy of $>100\ \mu\text{m}$.^[18] The main advantages of the FDM method in tissue engineering applications are its simple employment, rapid printing capability, diverse synthetic biomaterial availability, and favorable mechanical properties make it suitable for hard tissue regeneration applications. This technique also eliminates the need for solvent submersion and has the ability to fabricate large-format objects positively impacting scalability. Several synthetic biomaterials such as poly(caprolactone) (PCL), poly(lactic acid) (PLA), polyurethane, and their derivatives have demonstrated adequate thermoplastic performance and biocompatibility.^[58] Any biomaterials that can be melted and then re-solidified or thermally cross-linked are suitable for FDM printing.^[66] Exploiting low-temperature thermoplastic biomaterials is preferable in that biologicals can be added through more mild processes after bio-printing, preserving their functionality. Moreover, in order to offer a higher and more uniform strength between each layer, a conversion from thermoplastic material to thermoset material can be conducted via an additional crosslinking reaction using ionizing radiation or novel material design.^[67] The disadvantages are the limited material selection related to thermoplastic polymers and it is not suitable for printing with cells due to the high

manufacturing temperature. Therefore, an extra step is required after the FDM printing to seed cells on constructs for tissue/organ regeneration.

2.2.2.2. Laser-Based Acellular Bioprinting (LAB): Stereolithography techniques can also be applied for fabrication of acellular scaffolds. In these cases, however, more photocuring resins and crosslinking conditions are available since acellular constructs eliminate the concern of cell damage during the printing process. The increase in material selection is beneficial in that it allows for more diverse scaffold properties. Selective laser sintering (SLS) is another laser based printing technique that uses a high power laser for powder sintering, forming solid 3D structures on the surface of a powder bed.^[21,31,68] The technique relies on two energy sources, a bed-heater and a high-power laser. First, the particles are preheated between their melting transition and the temperature necessary for recrystallization during the cooling cycle. Localized thermal sintering of the particles is achieved by the controlled additional energy input of the a high-power laser, which traces the 2D layer design fusing exposed particles together within the layer as well as connecting it to the previously scanned underlying layer.^[37,68] This process may be printed using several material types such as ceramics, metals, polymers and their composites.^[68] Printing parameters, such as energy source, particle size, particle shape, free packing density, and thermodynamic variations of materials play critical roles in the fabrication process. The resolution of the different SLS machines usually ranges from 20 to 100 μm ; this is achieved and manipulated through a careful balance between therefore we need to consider a balance between obtaining fine resolution and allowing for adequate powder dispensability.^[68] The un-sintered powder serves as the physical support during 3D manufacturing, and unused powders may be removed or recycled after bioprinting. For polymer powder sintering, the laser parameters of power, beam size, scanning speed and spacing needs to be carefully controlled to avoid polymer degradation by overheating.^[68]

Selective laser sintering is applied to rapid scaffold prototyping in much the same fashion as in the industrial fabrication of metal or plastic components. The main advantages of this process for tissue engineering applications are the wide range of available biomaterials. Specifically, ceramics and metals are suitable to the fabrication of hard bone replacements or structural-supporting materials.^[68] Moreover, the powders used in this technique are more readily available than FDM materials, which are limited by filament prefabrication. Compared to other 3D printing techniques, the SLS is more expensive, cumbersome, and provides low resolutions for tough, stiff grafts. Additionally, material oxidation, thermal degradation, material shrinkage, and crystallinity change are concerns about material properties affected by the heating process that must be considered in fabrication.^[69] Additionally, a range of fillers can also be incorporated into the powder to further modify the appearance and properties of the printed parts. Being analogous to the SLS approach, a technology known as selective heat sintering (SHS) utilizes a thermal print head rather than a laser to fuse the surface of powdered thermoplastic materials into patterned, layered structures.^[31]

2.2.3. Recent Developments in Bioprinting Techniques—A recent development in SLA-based 3D printing involves continuous liquid interface production (CLIP), which is

facilitated through a well-controlled oxygen inhibited dead-zone (persistent liquid interface) preventing the resin from attaching to the UV window.^[21,58,70] Traditional SLA techniques use the bottom-up building approach and therefore require slow solidification to inhibit the adhesion process. CLIP, on the other hand, employs an oxygen-permeable curing window (a thin, amorphous Teflon film) below the UV image projection plane to create an oxygen-containing zone between the solid part and the liquid precursor where solidification cannot occur.^[58] The rate of resin replenishment in this dead-zone, the initiation efficiency, and the resin reactivity all combine to determine the rate at which the part can be formed in a continuous, rather than layer-by-layer, fashion. This approach allows 3D constructs production in minutes instead of the hours required with traditional SLA, and generates structures tens of centimeters in size that could contain features with resolutions below 100 μm . The choice of photocuring resins is fairly broad in CLIP; the viscosity and reactivity of the monomers, however, are more critical since they affect the oxygen diffusion within the resin affecting the permeable curing window.^[70]

3D powder printing is a powder-based 3D bioprinting technique that has been developed based on the principles of SLS.^[31,71–73] This technology uses a binder solution, such as water, citric acid or phosphoric acid, among others, to selectively bind the loose powdered biomaterial together in the designed geometry. Available biomaterials for binder integration include starch, dextran, gelatin, calcium phosphates, and hydroxyapatite among others.^[31,71,74] This process is reasonably inexpensive compared with other modalities, and provides more options for tissue engineering and drug-delivery because it avoids the damage of incorporated bioactive components. A major limitation of this system is the difficulty in removing unbound powder from desired hollow spaces. In addition, the usage of aqueous binding agents exhibits limited mechanical strength and resolution, and requires further post-processing. This technique is also difficult for direct depositing or patterning living cells. Several researchers are also using the inkjet printer to eject the binder droplet. This concept is closer to the traditional 2D inkjet technique where the powder bed acts like the paper.^[31]

A nano-stereolithography technique, also called two-photon polymerization printing (TPP), is used to photocure the liquid polymers by simultaneous two-photon absorption.^[75,76] Unlike the single photon polymerization process in SLA, two-photon polymerization allows electron transitions over excited energy levels; the polymerization process occurs when an atom absorbs two photons simultaneously. More specifically, a specific photoinitiator that reacts at low wavelengths simultaneously absorbs two photons with high wavelengths, their energies combine to achieve the energy of one photon with low wavelength and thus initiate the polymerization process.^[76] The photopolymerization that is triggered by nonlinear excitation happens at the focal point, but other regions are not affected by the laser energy. So it has the potential to print precise 3D structure with very high resolution, and even enable 3D construct printing inside the photocuring material solution without affecting other regions. This technique can achieve spatial solidification with a resolution of up to 100 nm.^[22] By exploiting the high resolution of this technique, many researchers have focused on the realization of 3D environments for cell adhesion and proliferation. Two-photon polymerization printing is an improvement, but the process and cost of materials often limits products to a small scale.

3. Material/Cells in 3D Bioprinting: From Bioink to Modular Building Blocks

3.1. Design and Selection Principles of Bioink

In addition to the bioprinting techniques chosen for the targeted tissue requirements, appropriate bioink selection, including cells, biomaterials and biochemical signals, is necessary for the successful construct fabrication. As printing and fabrication depend on the solidifying kinetics of the biomaterials and the native, chemically, or environmentally induced material properties, specific concerns arise based on the deposition mechanism and printing modality as discussed above.^[77] The bioink material is crucial because it should provide the spectrum of biochemical (i.e., chemokines, growth factors, adhesion factors, or signaling proteins) and physical (i.e., interstitial flow, mechanical and structural properties of extracellular matrix) cues which promote a favorable environment for cell survival, motility, and differentiation.^[10] Strategies for bioink selection can be divided into two categories: functional scaffold bioprinting (biomaterials with/without cells as the printing ink) or scaffold-free bioprinting (only use cells as the printing ink).^[20] In this section, we focus on the design strategies of bio-materials for functional scaffold bioprinting; scaffold-free bio-printing will be introduced in detail in section 3.5.

Generally, biomaterials range from cell supportive soft hydrogels, to stiff metal or ceramic implants and from nanoparticles and quantum dots for drug delivery and imaging, to complex functioning medical devices.^[16,50,78–80] In tissue engineering, the scaffolds fabricated by biomaterials serve as extra-cellular matrix (ECM) biomimetic structures that organize the tissue regeneration, temporary substitutes for tissue functions, and guides for regenerating tissue ingrowth or integration within a host tissue. Some basic elements including porosity, interconnectivity, pore dimensions, internal geometry, biodegradation kinetics, mechanical properties, and biocompatibility are also taken into account in the scaffold manufacturing process. Therefore, material science and/or engineering play crucial roles in programming an active and effective building block for tissue formation.

3.1.1. Design Principles—The design principles can be combined into four major considerations for selection (Figure 3):^[22,38,50,52,75,81] (1) Biomaterials must have suitable properties to meet specific bioprinter deposition requirements (printability). Printability refers to the capability of the material to support manufacturing and rapid solidification, the printability and interrelation of bioinks in various bioprinters and on associated substrates must be evaluated carefully to produce accurate, high-quality patterns. (2) Biomaterials must possess suitable physicochemical properties, including wetting/swelling, internal and external structure characteristics range from nano- to macro-scale, degradation kinetics, mechanical strength and structural stability. (3) Biocompatibility and biological activity are necessary for tissue development and remodeling over long-term in vivo implantation. The bioink material should facilitate engraftment with the endogenous tissue without generating an immune response and provide a spectrum of biochemical cues (i.e., chemokines, growth factors, adhesion factors, or signaling proteins) that promote an environment for cell survival, motility, and differentiation. (4) The materials should be affordable, abundant, and commercially available with appropriate regulations for clinical use.

3.1.2. Bioink Formulations—Acellular 3D bioprinting technologies, including the deposition of metals, ceramics and thermoplastic polymers, generally involve the use of organic solvents, high temperatures, crosslinking agents or other severe process conditions. As such, an extra post-process step such as purification, sterilization, or other modification is necessary for further biomedical application.^[21,78] In contrast, cellular bioprinting requires biocompatible fabrication processes and biomaterials during printing, ensuring cell viability and development throughout. Therefore, Food and Drug Administration (FDA)-approved biomaterials are preferred in these applications; the biocompatibility evaluation for newly developed materials and their degradation byproducts needs to be performed in vitro or/and in vivo before gaining approval.

In general, the printable biomaterials are divided into two categories:^[22,38,50] (1) Hard biomaterials, such as metals, ceramics, and curing (thermoplastic) polymers. They can fabricate mechanically robust and durable constructs. These materials typically require high temperatures or toxic solvents to facilitate printing, so that they are not appropriate for printing together with cells. Therefore, cells are usually seeded onto the printed constructs after fabrication, avoiding conditions harmful to the cells. A dynamic cell seeding method is often utilized to improve scaffold coverage. The interconnectivity of pores allows for uniform cell distribution. (2) Soft biomaterials such as hydrogels, comprised of synthetic or natural polymers, possess biomimetic characteristics, providing a favorable environment for cells. The cellular bioprinting technologies currently available are only capable of dispensing liquid materials or hydrogels (they should be in liquid or paste-like form during printing). In order to better mimic the properties of natural ECMs, many biomaterial combinations have been designed for cell printing mimicking the mechanical properties and bioactivity of native tissue. Moreover, the more specific and complex printable materials are steadily being developed to match desirable traits for a variety of biomedical application.

In addition to the components of bioink, the resultant formation is also an important factor. For example, extrusion-based and SLA-based bioprinting are very versatile in depositing a wide array of bioink types, including hydrogels, microcarriers, tissue spheroids, cell pellet, tissue strands and decellularized matrix components. Extrusion-based bioprinting also is capable of depositing small building blocks in a fugitive liquid delivery medium, remains flexible in nozzle tip design, and has the ability to extrude bioink in near solid state, due to larger nozzle diameter ranges.^[50]

3.1.3. Solidification Mechanisms—Some general types of curing approaches are described in Figure 2.^[38,50,52,81] The curing methods of hard biomaterials can be easily understood. (1) The melt-deposition is based on phase transition of associated materials around their melting point. (2) The solution-deposition is mainly used in curable polymers. The proper organic solvents (volatile or exchangeable) need be chosen to dissolve the different polymers. For soft biomaterials, cell-laden hydrogel solutions are the most typical or universal bioinks. Various key properties such as concentration, molecular weight, viscosity, gelation kinetics, and stiffness are important determinants. The solidification (or gelation) mechanisms include physical crosslinking and covalent crosslinking. As one of the typical physical crosslinking methods, a phase transition from sol to gel state can be controlled by the printing environment change (various external stimuli) such as

temperatures, pH, or others. The ionically cross-linked network is formed via multivalent counterions, however, these ions could be leached out or exchanged by other ionic molecules in long term culture, compromising the control over the construct properties. Other physical interactions such as hydrophobic, electrostatic, hydrogen bond, or inclusion complex can employ the solidification of 3D structures, however, their weak mechanical strength limits their application. Therefore, covalent network formation is preferred in order to enhance the mechanical stability. In general, the radical based cross-linking can be induced by light, redox, and temperature; the non-radical crosslinking methods involve Michael addition, enzymatic, glutaraldehyde, carbodiimide, and genipin among others, so the toxicity of the crosslinking agents should be considered. In the light-induced deposition or solidification strategies, the photoinitiators or photosensitizers are commonly applied to initiate the radical crosslinking reaction of monomers and/or pre-polymer solutions, such as D-p-chromophore (known for its high sensitivity in 2PP processes), Irgacure 2959 (I2959; high biocompatible initiator and UV working range), lithium acylphosphinate salt (LAP, biocompatible initiator and visible light working range), VA-086 (high biocompatible initiator and visible light working range), and camphorquinone (CQ; an initiator with many dental applications and visible light working range) among others. Some chemical crosslinking reactions are too slow to support 3D structures during rapid printing, thus multiple-step crosslinking offers a better choice. Normally, the printing temperatures of cells encapsulated in the hydrogels should be around the physiological temperature in order to avoid ice nucleation or overheating, which are harmful to cells. In vivo stabilities, permeability, compatibilities, and degradation rates of polymer hydro-gels should be seriously considered before the 3D constructs can be implanted, particularly for soft tissues or organs. In addition, the swelling and contraction characteristics of the bio-inks have to be considered so that deformation of the final construct can be prevented via the proper selection of bio-ink type.

3.1.4. Bio-Functionalization—An ideal scaffold should possess excellent bioactivity for regulating cell events. Directly encapsulating growth factors or cytokines into bioinks is a simple way of regulating cellular behaviors through diffuse release after bioprinting.^[82] Several conventional approaches can also be used to modify the printable biomaterials such as incorporation with bioactive factors, enzymatic recognition sites, and adhesion factors among others.^[12,83] The bulk modification before or during the printing process may affect the physicochemical properties of the resultant scaffolds, while post-processing surface modification on printed scaffolds only changes the interactions between cell/tissue and material surface.^[66,84–86] Based on the 3D printed biomimetic spatial structure, incorporating bioactive components into constructs provides the proper spatial distribution of biochemical cues for guiding tissue formation and remodeling.^[82,87] Herein, the surface modification involving physical adsorption or chemical conjunction has been widely utilized to increase cell attachment, proliferation and regulate cell differentiation by means of interacting with cellular surface ligands and/or modulating the signaling pathways.^[6,86,88] Moreover, the presence of nanoscale features also affects cell adhesion, cell orientation, cell motility, and cytoskeletal assembly.^[8,11] Other techniques such as microspheres or hydrogels can be combined into 3D bioprinted scaffolds to achieve efficiently sustained release of various bioactive factors.^[89] The strategies to engineer biomaterials with specific physiological functions requires a comprehensive understanding of the complex biological

mechanisms of the regeneration process, involving the natural tissue-specific composition, the localization of bioactive components in ECM, and the complex cascade of signaling pathways in normal physiological events.

To date, the exploration of new biomaterials for tissue/organ bioprinting is still underway. Emphasis should be given to those printed scaffolds that play a significant role in cell survival, proliferation, migration and differentiation during and after bioprinting processes. They also must possess the principal means of mechanical support and biochemical signals for the long term tissue regeneration. Due to the limitations of material properties relative to specific printing techniques, 3D constructs with complex structures and characteristics were difficult to realize.^[7,20,65] Therefore, multiple printing techniques or material systems can be integrated into a 3D construct by choosing the proper printer and materials with appropriate printability. Combining 3D bioprinting platforms and techniques has been proven to be an effective alternative, especially for complex organ manufacturing.^[87]

The inherent characteristics of these different printing materials, including solubility, viscosities, melting points, mechanical properties, and available chemistries for crosslinking and functionalization are responsible for the overall success of the design. More importantly, the customized approaches described above will provide potential strategies for creating versatile materials to support successful bioprinting.

3.2. Common Bioinks and Recent Developments

Currently, most research focuses on the development of new printing techniques, the update of printing parameters (resolution, speed or others) or the bio-application of printed constructs instead of exploring new printable materials and their functionalization. Therefore, the lack of variety in ideal, printable biomaterials remains a major challenge. The different printing techniques have specific requirements for the properties of bioinks as we discussed above. In this section, we will briefly cover the traditional and universal biomaterials used in bioprinting, and will further discuss the development of new printable biomaterials.

3.2.1. Hard Biomaterials (Metals, Ceramics, and Thermoplastic Polymers)—In the field of tissue engineering, hard biomaterials are derived either from natural or synthesized materials, containing in metallic components, polymers, ceramics or composites.^[21,31,78]

Metals have been used clinically for bone replacement or repair in the biomedical community because of their high mechanical strength and in vivo safety.^[21] Common metals such as stainless steel, titanium, and certain alloys have been studied in 3D printing as well, and some have progressed to clinical trials.^[68,69] However, limited 3D metal printing techniques, metal corrosion and ageing, and potential toxicity of metal ions are serious considerations being further evaluated for long term implantation. Biodegradable implants are preferred for tissue regeneration, thus a “biodegradable metal” concept has been proposed.^[90] Some magnesium-based, iron-based, zinc-based, or other biodegradable metal-based composites, which consist of the pure metals themselves, alloys, or metal matrix composites have been reported.^[90] The favorable biocompatibility, suitable degradation

rates, and completed metabolism can be observed in studies either in vitro, or in vivo. As the availability of biodegradable metals increase, more comprehensive research is needed before further clinical applications can progress.

Ceramics and glasses are widely used as biocompatible materials for dental, joint and bone implantation due to their mineralization abilities.^[72,91] Therefore, bioceramics containing both metallic and nonmetallic elements are applied in the 3D bioprinting field ranging from ceramic oxides (inert in the body) to resorbable materials (eventually replaced by regenerated tissue).^[92] Hydroxyapatite (HA) is a primary component in human teeth and bones. It, along with its analogues tri-calcium phosphate (TCP) and calcium phosphate (CaP), has been printed into bone scaffolds with biomimetic structures, adequate mechanical strength, and the ability to promote osteogenesis.^[93]

The physicochemical and mechanical properties of synthetic polymers can be easily modified for enhancing tissue engineering outcomes, and these materials can be produced at low cost without immunogenicity. Some FDA-approved degradable polymers and their copolymers are extensively used in FDM and SLS bioprinting.^[22,31,81] Polycaprolactone (PCL) and poly lactide (PLA) are the most widely used biocompatible and biodegradable polymers used with FDM because of their proper melting temperatures and good solubility allowing easy printing and processing.^[78,79] In addition to being used for fabricating tissue engineering scaffolds, they can also be used as a 3D structural support for cell-laden soft materials in the printed constructs. PCL, however, exhibits very slow degradation, due to its semicrystalline structure, hydrophobicity, and low water absorption capacity. Poly(lactico-glycolide) (PLGA) is another material that is ideal for extrusion bioprinting; degradation can be controlled by adjusting the polymerization ratio between the lactide and glycolide groups, another favorable feature of this material. Poly(3-hydroxybutyrate) (PHB) is a natural thermoplastic polyester produced by microorganisms that has also attracted attention for 3D bio-printing applications. Acrylonitrile-Butadiene-Styrene copolymer (ABS) is not widely used in medical devices in comparison to biomaterials such as PCL and PLA which offer greater native biocompatibility. Although surface modification has been applied to engineer hydrophilicity and enable biocompatibility, it shows limited promise for biomedical application. Variations in the copolymer structure and polymer concentration enable the tailoring of mechanical properties for the scaffolds.

3.2.2. Soft Biomaterials (Hydrogels)—With the exception of the stiffest tissue types such as bone and teeth, hydrogels can recapitulate a range of elastic modulus values through manipulation of chemistry, crosslinking density, and polymer concentration, thus mimicking the elastic moduli of most soft tissues in the body.^[14,50,94] Soft biomaterials mainly used in the cellular bioprinting techniques are predominantly based on either naturally occurring polymers and their derivatives (including alginate, gelatin, collagen, chitosan, fibrin and hyaluronic acid, often isolated from animal or human tissue) or synthetic materials (polyethylene glycol (PEG), Pluronic F127 and their derivate copolymers, includes polyesters, polypeptides or others).^[21,65,79,81] The advantages of natural polymers are their similarity to human ECM, and their inherent bioactivity, however, they are limited by immunogenicity, weak mechanical strengths and a lack of control in composition/molecular weight. The advantage of synthetic polymers is that they can be tailored with specific

physical properties in terms of tissue response such as specific molecular weight, chemical structure, composition and functional group chemistry as well as bioactive anchored sites (i.e., adhesion motif or enzyme degradation sites) to suit particular applications.^[50]

As the synthetic polymers, both polyethylene glycol PEG and Pluronic F127, are water-soluble polymers, they are intensively used as a representative sacrificial material for fabricating complex 3D constructs.^[50] Pluronic F127 is of particular interest because it possesses the characteristic of thermo-reversible gelation dependent on the solution concentration. Pluronic F127 can transform from a liquid under 4 °C to a gel at over 16 °C when above 20% w/w concentration. Both PEG and Pluronic F127 should be chemically modified prior to forming physical or chemical networks when using as tissue engineered scaffolds.^[95] The typical method for achieving gel formation is acrylation or methacrylation, where the chemically modified PEG or Pluronic F127 is generally crosslinked under UV exposure. Additionally, their derivative copolymers including polyesters and polypeptides, among others, have been widely synthesized as physical or chemical hydrogels and used for cell encapsulation, which can also be applied in 3D cellular printing and manufacturing.

Natural polymers and their chemical modifications are the most widely used as printable biomaterials and encapsulating living cells due to the similarity of their components to the native tissue microenvironment.^[20,50,81] They can also provide tissue-specific biochemical and physical stimuli to guide cellular behaviors including migration, proliferation, differentiation, and maturation. For use in bioprinting, natural polymers have been employed in several ways, to include the use of the temperature sensitivity or ionic interaction characteristics to facilitate extrusion, and the use of covalent addition of functional groups to induce chemical crosslinking approaches.

Alginate (Alg) is an anionic polysaccharide derived from algae or seaweed.^[96] This material is composed of two repeating monosaccharides (i.e., L-guluronic and D-mannuronic acids), therefore, the typical ionic hydrogel can be formed using multi-valent cations (i.e., Ca^{2+} , Zn^{2+}) instantaneously, making it attractive for 3D tissue/organ printing.^[96,97] The crosslinking processes are reversible, however, so the printed structures cannot be maintained for long-term culture applications.^[96] Hyaluronic acid (HA), or hyaluronan is a linear polysaccharide component of the ECM (non-sulfated glycosaminoglycans), which has been used clinically for several decades for treatments such as therapy for damaged joints and arthritis.^[98] Acrylate or methacrylate modified HA can be crosslinked to form a hydrogel via light based 3D bioprinting. Thiol-modification of HA can form a hydrogel through Michael-type addition reactions with active vinyl based crosslinkers.^[38] Limitations of HA as a bio-material for bioprinting are that HA hydrogels are typically too soft to form robust structures, and show significant swelling behavior. Collagen (Col) is a main structural protein of ECMs; it responds to simple crosslinking via thermosensitive gelation under physiological conditions, which can be a major advantage in 3D printing.^[99,100] However, the high cost and weak mechanical strength limit its application. Gelatin (Gel) derived from partially hydrolyzed Col is inexpensive, and also possesses thermosensitive properties.^[101] Both Col and Gel have abundant proteins including fibronectin, vimentin, vitronectin, and arginine-glycine-aspartic acid (RGD) peptides, which promote cell adhesion. The transition temperature of Gel lies around 30 °C limiting its direct application as the cell scaffold at

physiological temperature, thus it commonly serves as the sacrificial material in 3D printed structures.^[50] The reversible gelation mechanism in aqueous conditions is based on the formation of an alpha helix structure below 30 °C and a random coil structure above 40 °C. Gelatin methacrylate (or gelatin methacrylamide, GelMA) has been widely used to fabricate scaffolds via the various light-based printing platforms.^[102] Additionally, the aforementioned thiol-ene crosslinking method has also applied to the GelMA system when adding thiol-based materials.^[94] Fibrin is comprised of fibrinogen monomers that are cleaved with thrombin by a blood coagulation crosslinking mechanism, thus fibrin plays an important role in the blood clotting and wound healing processes.^[103] It is widely used as surgical glue in high concentration, or cell scaffolds in low concentration, due to its rapid gelation property. However, the fibrin hydrogel is too soft and fragile to maintain a 3D shape.^[104] Decellularized extracellular matrices (dECM) from different tissues contain a variety of proteins, proteoglycans and glycoproteins of native tissue ECM components, so it has been used as bioink capable of recapitulating a tissue-specific microenvironment in printed 3D tissue/organ analogues.^[100,105,106] Challenges in tissue decellularization are with ensuring the complete removal of cellular components while maintaining of the fine vasculature and other tissue structures.^[107] Additionally, some toxicity has been observed when cells are grown on decellularized tissue scaffolds, potentially due to the retention of the decellularization detergent.^[105] Other natural polymers such as starch, cellulose, and dextran, among others, have been developed for 3D printing scaffolds with potential use in tissue engineering or other biomedical applications.^[22,38,50,65,79,80]

3.2.3. Latest Development of Bioinks—The chemical modification of biomaterials may provide a promising approach for extending 3D printable bioinks.^[65,77,94] For example, the photocrosslinkable macromers or prepolymers can easily be prepared by acrylated/methacrylated multi-armed oligomers/polymers or branched polymers. Photocrosslinked networks have a high gel content, which indicates a high degree of crosslinking. However, due to the solvents used in these systems, shrinkage or swelling of scaffolds may occur after drying or soaking, resulting in changes in structural and mechanical properties. Some macromers can be heated above the melting temperature to obtain the suitable viscosity; in such cases, no solvent is needed for bioprinting and no obvious material shrinkage is observed after cooling. Additionally, other covalent crosslinking systems have been developed in the 3D printable inks. A thermally reversible dynamic covalent Diels–Alder reaction was used to synthesize a printable PLA blend for dramatically improving both strength and toughness of the scaffolds.^[67]

Currently, composites of polymers and bioactive materials are being developed with the aim of increasing the mechanical scaffold stability or improving tissue interaction.^[21] The composite scaffolds combining a variety of biodegradable polymers and bioactive ceramics are fabricated by 3D printing and are capable of achieving high mechanical strength and good biological activity. Generally, the stiffness of the cured composites will increase with raising the concentration of nanoparticles or other materials. Synthetic polymers can often be combined with bioactive materials, naturally derived materials or other functionalized materials to create more complex hybrid structures.

Moreover, the strongly desired characteristics of advanced tissue scaffolds involve both biomimetic properties in structure and the ability to regulate cell behavior.^[7,94] Engineering techniques that mimic the critical aspects of natural healing and growth cascade are preferred to augment the proliferation and differentiation of the recruited or implanted cells; this is often achieved through the integration of growth factors and cytokines that provide suitable biochemical and physicochemical factors for tissue regeneration. Engineering these dynamic ECM mechanisms into biomaterials offers further control over cell behavior. One challenge is in developing methods to incorporate these biologically inspired materials into constructs using bioprinting technology. Material printability and degradation characteristics such as time and byproduct emission must be better understood for progression toward clinical applications. Also, it is essential that these materials have well-understood and controllable structural and functional biological effects before advancing to in vivo testing and application.

3.3. Cell Sources and Selection

The choice of cells for tissue or organ printing is crucial for functionality of the fabricated construct, especially for future clinical application.^[108] Tissues and organs are comprised of multiple cell types with specific biological functions that must be recapitulated in the regenerated tissue. In addition to the primary functional cell types, most tissues contain various cell types that provide supportive, structural or other functions, or are involved in vascularization or provide an essential surrounding for functional maintenance and development of the primary cells.^[20] Therefore, the options for printing cells not only involve the arrangement of primary cell types in the 3D printed construct, but also have a close relationship with other cells for contributing to complete functionality of complex tissues/organs.

3.3.1. Principles of Cell Selection—Cells used for 3D printing should take into account several elements.^[16,20,81] (1) Sufficient numbers of cells can be expanded in vitro culture for bioprinting; (2) Cells must be robust enough to survive during or after the bioprinting process; (3) Appropriate cell proliferation and controllable differentiation in the 3D printed scaffolds are required for either in vitro culture or in vivo implantation; (4) Cellular functions can be maintained in vitro to closely mimic the true physiological state, and developed after implantation by stimulation with the in vivo environment, including physical forces and biological stressors; (5) Physiological specificity both structural and functional on different cell types; (6) Interaction of multiple cells for tissue development involves biological signal paths.

3.3.2. Cell Sources—In order to maintain long-term function after implantation, the bioprinted construct must be able to maintain cellular homeostasis, self-renew, respond to tissue damage or injury, and integrate with host tissue or organ.^[16,20]

Host immune response may be triggered by the implantation of exogenous cells. Therefore, the autologous source of cells is the preference, autologous cells may be obtained from the patients themselves through the generation and differentiation of autologous stem cells or through reprogramming approaches, to avoid negative immune responses. However, some

limitations make it difficult to apply autologous cells in bioprinted constructs for tissue regeneration. Examples of these challenges are: technique restrictions on the isolation and in vitro culture of cells, finite expansion or regeneration capacity of many primary cell types, and the effectiveness of patient-sourced cells. Pluripotent stem cells including embryonic stem cells (ES) and induced pluripotent stem cells (iPS) are promising cell types due to their ability to proliferate in an undifferentiated but multipotent state (self-renewal) and their capability to generate multiple functional tissue-specific cell phenotypes.^[20,38] Especially, iPS derived directly from adult tissues requires reprogramming the cell type thus overcoming the difficulty and limitations associated with the current cell sources. Adult mesenchymal stem cells from bone marrow, fat, umbilical or other sources can differentiate into osteoblasts, chondrocytes, adipocytes, cardiac cells, endothelial cells, smooth muscle cells, hepatocytes, and neural cells and can be used in many biomedical applications. Although they have a more limited multipotent differentiation potential, they are considered safer for clinical uses and show great promise for bioprinting applications. According to previous studies, high cell viability can be obtained through optimizing the printing parameters; overall the printing processes have no adverse effects on the stem cell proliferation and differentiation abilities.^[50]

The 3D printed constructs for the complex tissue or organ regeneration need to be fabricated with either functional primary cells with supporting cells or progenitors/stem cells for further differentiation.^[16,23,26] In cellular printing, multiple bioinks with different cells need to be prepared to print in parallel, requiring complicated and precise control of the printing step. Additionally, acellular printing is difficult to post-seed specific cells on the desired regions of complex 3D structure. Printing stem cells with the regional bioactive factors, or post-seeding stem cells on the construct with the regional bioactive factors, may reduce the complication of the fabrication process for complex tissue/organ regeneration. Stem cells can be differentiated into target cell types by bioactive factors in the combination of location or spatial arrangement. Therefore, 3D stem cell printing can provide a simple and effective approach for regenerating complex tissue/organ.

3.4. Modular Fabrication of Mini-tissue

Regeneration of a tissue or organ including cellular and extra-cellular components, needs to reproduce specific cellular functions, thus a complete understanding of the tissue micro-environment, such as specific organization and hierarchy of various cell types, gradients and arrangement of biologicals, composition of the ECM as well as the native biomechanical stimulation in vivo.^[17] Tissues or organs can be considered as an aggregate structure consisting of small structural and functional components, which can be defined as functional building blocks.^[23,36,50] Modular fabrication of these building blocks can easily be assembled to complete tissues. 3D bioprinting techniques can be used to print these building blocks and guide them to assemble into 3D living structures. The process of tissue/organ development relies on cellular self-organization through direct assembly in scaffold-free conditions or aggregation along with the 3D printed scaffold degradation.^[20] This spontaneous self-organization happens during development in vivo, but has also been recapitulated in numerous in vitro applications.

In addition to the traditional “cell-scaffold” approach, cell aggregation is a typical technique of tissue fabrication, in which solid cellular units are directly used as building blocks to engineer the tissues.^[23] This technique enables scaffold-free bioprinting, even free of exogenous biomaterials. The concept originates from the knowledge of developmental biology and the fact is that, tissues and organs are formed without any scaffolds during embryonic development. Generally, cellular aggregation techniques have some typical procedures: (1) Cell expansion; (2) Initiation of cell aggregation; (3) Cellular pellet collection; (4) Geometric molding, such as cylinder or spheroid.^[20,23] Moreover, the multiple cell types can also be organized during cell aggregation, especially endothelial cells can be co-cultured to form vascularized cellular aggregates.^[109] After obtaining sufficient mechanical integrity, aggregates with diameters ranging from 200 to 500 μm can be printed as building blocks to form 3D structures. However, the directly printed constructs are fragile and lack cohesive tensile strength. Therefore, successful fusion is a very important process for the formation of 3D structures that rely on the cohesive ability of multicellular aggregates and additive properties. The accumulation of ECM, associated restriction of cell motility and enhancing tissue cohesion in tissue spheroids can change kinetics or impede the tissue spheroids’ fusion process.^[23]

One advantage of this technique is potentially accelerated tissue organization and the ability to direct the formation of complex structures.^[23] Tissue spheroids are thought to possess material properties that can replicate the mechanical and functional properties of the tissue ECM. Moreover, by manipulating the host bioactive composition, self-organization can be controlled. Unlike the critical role of bioinks in assisting the ECM production in traditional 3D bioprinting, bioprinted self-assembling cellular spheroids may produce a suitable ECM environment by themselves.^[17,23]

It is noteworthy that in either biomaterial based bioprinting or scaffold-free bioprinting, cell-laden bioprinting techniques require suitable nutrient and oxygen transport for regenerated tissues/organs through proper pore architectures or vasculature analogues.

4. 3D Bioprinting of Organs

4.1. Definition, Elements and Procedure

3D bioprinting of organs is a comprehensive or integrative approach that offers a pathway for scalable and reproducible mass production of engineered living organs.^[35] It allows the precise simultaneous 3D positioning of multiple cell types with high density to mimic their natural counterparts.^[110] More importantly, it enables the creation of functional complex tissues with vasculature and neural networks.^[20] The ultimate goal is industrial, scalable, biofabrication of patient-specific functional 3D living human organs suitable for clinical implantation.^[15]

As previously mentioned, bioprinting techniques have the most tremendous potential on manufacturing the complex structures compared to all traditional tissue engineering techniques. Although avascular or thin tissue bioprinting has shown great promise in current research, complex tissue or organ bio-printing for implantation remains a challenge.^[16] Prior to recapitulating organ-level complexity, creating functional tissue is an essential stage that

contains a hierarchical arrangement of multiple cell types in a 3D microenvironment. This includes the primary functional cells depending on tissue type, along with a multi-scale network of vasculature in stroma and parenchyma, as well as lymphatic vessels and neural networks.^[4,17,26]

The requirements for 3D printing biological tissues and organs can be summarized in three elements: (1) Biomimetic structure (modeling and resolution); (2) Biocompatible and bioactive components; (3) Bio-microenvironment, either *in vitro* or *in vivo*, including biomechanics and biochemistry. The first two have been discussed in the technique and bioink parts of this manuscript. The various bioprinting techniques and bioinks can facilitate the hierarchical fabrication of multiple cell types and direct them to differentiate into desirable tissue types. The post-bioprinting process is crucial to provide an adequate bio-microenvironment including mechanical, chemical or biological signals to regulate tissue remodeling and growth.^[65] The development of new bioreactor technologies enables the rapid maturation of tissues, multiscale vascularization for survivability of tissues, and mechanical integrity and innervation for implantation.^[20,38] In complex tissue/organ bioprinting, the post-bioprinting process or the tissues/organ regenerated process involves three phases:

(1) Cell viability. For cellular bioprinting, the time of printing procedure and the sensitivity of cells may impact the cell viability. If the time is long and the cells are fragile, then without any supplement of extra nutrition, the cell viability will decrease severely. Therefore, the bioprinting time, including preparation time, should be shortened; the incorporation of culture media during printing can also significantly improve cell viability.

(2) Mass transport and mechanical stimulation. The cells are directly encapsulated in the bioinks in the printing process or are post-seeded onto the printed constructs; it is essential to supplement them with nutrients and oxygen during the culture periods. After fabrication, the constructs with viable cells must not only remain viable for the long culture period, but also must be able to function as intended. Bioreactors, typically employing perfusion, tensile or compressive loading, rotation or other conditioning, may provide a dynamic surrounding and mechanical stimulation for cell culture *in vitro*, mimicking the native fluid environment and physical forces *in vivo*.^[38,65]

Shear forces created by medium flow through the 3D printed constructs facilitates efficient transfer of nutrients and oxygen. This perfusion system can be used to mimic haemodynamic forces and pressures that occur naturally in the human body thus improving ECM production and mechanical properties of the artificial tissues/organs.^[87] Compared with slow permeation in static culture, the use of a bioreactor, or direct implantation *in vivo*, could be more beneficial for ensuring homogenous and efficient mass transport.

Furthermore, the mechanical cues, present at the onset of several signaling pathways in normal physiological conditions, have been known to positively influence tissue formation and further integration.^[111] In addition to the intrinsic mechanical stimulation from biomaterial composition, periodic stretching, pulsing, or

compression that mimics the physical forces its corresponding tissues or organs experience in vivo can increase strength and flexibility, as well as increase matrix reorganization and maturation of the construct.^[38]

(3) Construct maturation. In this stage, the cells must proliferate to form the appropriate cell-cell connections for communicating with each other; they must be able to secrete their own matrix components and perform natural biological functions, further integrating into the host tissue. The phenomenon involved in maturation that was discussed above can be accelerated using techniques such as mechanical conditioning. The constructs may provide an appropriate environment for cell development, both biomechanically and biologically, and can also be replaced by deposited native ECM with increasing time. Over time, cells reach equilibrium states between cell–matrix adhesions, such as integrins, and cell–cell adhesions, such as tight junctions and adherens junctions. These interactions between cells and cell–matrix offer the ability of cell populations to spontaneously reorganize into 3D tissue.^[38]

After in vitro maturation of 3D printed constructs, the engineered tissue needs to be implanted into the patients' body for in vivo integration. This phase will involve the issue of bio-manufactured construct immune acceptance, in vivo safety and efficacy, and monitoring of construct integrity and function post-implantation.^[16,20,50]

Therefore, as mentioned above, several challenges must be progressively addressed to make organ printing become a reality. The most critical challenge is the integration of a vascular network and a neural network in the 3D printed constructs, which is also a problem the majority of tissue engineering technologies are facing. In the following section, we will present recent developments on bioprinting scale-ups of complex tissue and organ constructs for implantation, including vasculature/vascularized tissue, neural regeneration, and organ constructs. We will also discuss major roadblocks toward clinical translation and provide potential solutions and future perspectives.

4.2. 3D Bioprinting Applications in Organ Regeneration

4.2.1. Vasculature—To maintain metabolic functions, the native tissues or organs require the supplementation of adequate nutrients, gas exchange, and metabolic waste removal, all of which are also necessary for engineered tissue maturation.^[112–114] Without these, low cell viability and malfunction of artificial tissues/organs may result, especially when scaling-up tissues with a high volumetric oxygen-consumption rate, such as cardiac, pancreatic, or liver tissue. Vasculature within the tissues or organs is crucial for transporting oxygen and nutrients and maintaining tissue functions.^[113] Cells existing more than 200 μm away from the nearest capillaries will undergo hypoxia, apoptosis and ultimately cell death, due to limited diffusion ability.^[112] Therefore, the most critical challenge for complex tissue and organ regeneration is the integration of a vascular network, which is also a major problem in 3D bioprinting of complex tissues and organs.^[26,109,110,115]

Native blood vessels have complex unique structures in multi-scale and multilayer arrangements. The inner diameter of blood vessels ranges from microscopic size, 5~10 μm

for the smallest capillaries, to 30 mm, for the largest artery (aorta).^[116] Walls of the large vessels, namely elastic arteries, muscular arteries and veins have three distinct layers starting from the vessel lumen: intima, tunica media and tunica adventitia respectively.^[117,118] Intima, the innermost layer is a thromboresistant confluent monolayer of ECs and is attached to a basement membrane (40~120 nm). Media, the middle layer, is comprised of a dense population of concentrically organized SMCs with bands or fibers of elastic tissues, and adventitia, the outermost layer, is a collagenous ECM containing mainly fibro-blasts and perivascular nerves.^[119] In contrast, the capillaries only consist of EC layer. Although grafts can spontaneously vascularize after implantation (involving an inflammatory wound-healing response and hypoxia-induced endogenous release of angiogenic growth factors), the process of angiogenesis and inosculation with microcirculation in vivo is too slow to provide sufficient nutrients and oxygen to the cells inside of the tissue construct.^[120] Obtaining a functional vasculature, consisting of adequate vessel geometries and dimensions through 3D bio-printing strategies, is absolutely essential.^[112,118,121]

Encapsulating ECs or SMCs into bioprinted constructs without perfusable channels has developed for self-assembly of interconnected vasculature.^[122] This method of generating blood vessels in artificial tissue relies on the ability of ECs to organize into blood vessels autonomously (angiogenesis), thus only capillaries can be created. Although such designs lead to the formation of vascularized tissue, capillaries are too far from the arteriovenous (AV) loop and the tissue, in vivo, was prone to necrosis after longer implantation times. Additionally, from a tissue engineering standpoint, it is not necessary to consider the fabrication of the capillaries, because they can sprout from the large blood vessels based on the native angiogenesis process (a complex cascade of events including ECs activation, migration, and proliferation as well as arrangement). The rate of sprouting angiogenesis is around 1.0 mm per week in vivo. Compared to the commercial and clinical successes in large-diameter vascular grafts, manufacturing small-diameter (<6 mm) vasculature currently remains a formidable task.^[123]

3D bioprinting technology is currently unsuccessful in fabricating hierarchical and complex structural vasculature, where vascular trees spanning arteries and veins down to capillaries are required to be manufactured to mimic natural vascular anatomy.^[112,114] More importantly, successful maturation toward functional, mechanically integrated vasculature is still a challenge. The main unit of the vascular tree is a 'Y' shape branching unit (a bifurcated pattern); the repeat of multi-scale units will form a hierarchical structure with different branching orders.^[109,115] The constructs at submicrometer scale are difficult to be printed using the current techniques. Therefore, instead of fabricating a biomimetic vascular tree, some researchers alternatively print perfusable (bifurcated or branched) channels at micrometer or higher scale to mimic a vascular network, facilitating medium flow and oxygen supplementation for cell viability, tissue maturation and formation.^[87,95,124]

Here, we focus on the manufacturing of interconnected channels or free-standing tubular structures, allowing native blood vessel ingrowth and anastomosis. Over all, three approaches have been developed: (1) indirect bioprinting through utilizing sacrificial templates (a fugitive ink) that is removed to create hollow channels in a bulk construct; (2)

directly bioprinting interconnected channels in a construct; (3) direct bioprinting of a vasculature network or blood vessel in a tubular shape.

4.2.1.1. Sacrificial Templates: In indirect bioprinting, cell-laden hydrogels serve as the bulk matrix to fabricate vascularized tissue constructs; here the vascular networks are printed with fugitive inks. The endothelium lumen is generated inside tubular channels after the perfusion culture of endothelial cells (ECs). The integration of the vascular network shows significantly increased cell viability near the channel regions inside the construct compared with other deeper regions. In an earlier study, carbohydrate glass was used as a cytocompatible sacrificial template to print rigid 3D filament lattices.^[125] After crosslinking the ECM gels, the glass filaments were dissolved to form vessels with intervessel junctions. In co-cultures with 10T1/2 cells in the interstitial space, endothelial cells lining the vascular lumen became surrounded by the 10T1/2 cells and formed single and multicellular sprouts extending from the patterned vasculature into the bulk hydrogel (Figure 4a).^[125] Thermosensitive fugitive ink, Pluronic F127 was also explored to print microvascular networks (Figure 4b).^[95,124,126] After a cooling process, the perfusable channels possessed final diameters ranging from ca. 100 μm ~1 mm in the GelMA hydrogel (Figure 4c).^[124] In a thick osteogenic tissue model (>1cm thick and 10 cm^3 in volume), the embedded vascular network ensured uniform and long-term perfusion culture throughout the construct, promoting the osteogenic differentiation of encapsulated human mesenchymal stem cells (hMSCs).^[126] In other studies, a straight EC-laden gelatin line was printed inside of the collagen layers.^[127] The 3D printed constructs were incubated at 37 °C for 30 min to complete the collagen gelation and the gelatin liquefaction. The functional vascular channels and the sprouts were generated with fully covered ECs.^[127] Although the bioprinted sacrificial template method for vascular fabrication has exhibited feasibility, flexibility and angiogenic ability, this technique still faces some challenges. First, the fabricated vasculature only possesses endothelium and is unable to repeat the multilayer cell structure of native blood vessels. Additionally, the current studies only suggest the 3D printed channel could provide sufficient nutrients for cell viability inside of constructs, which is similar with the interconnected pores in the traditional scaffold design. The functionality and inosculation with microcirculation in vivo has yet to be systemically explored. Finally, the structure of vascular networks totally rely on the bulk hydrogel constructs, thus structural fabrication of external constructs is limited, such as the hierarchical structural design and the biomimetic distribution of multiple cells.

4.2.1.2. Direct Printing of Interconnected Channels: Direct bio-printing of a construct with interconnected channels is another approach to fabrication of vascularized tissue. For example, the millimeter-sized branched channels were designed and printed in poly(ethylene glycol) dimethacrylate (PEGDMA) hydrogels by SLA.^[128] In addition, a high-resolution μSLA technique was utilized to print 3D cell/biomaterial patterns with <5 μm resolution, as well as open fluidic channels with 100 μm diameter for angiogenic cell-encapsulating patches.^[63] Although laser based methods are capable of producing extremely high-resolution features and fluidic channels, architectural complexity is still largely restricted to uniaxial channels. The open channels would be crosslinked by light exposure after printing the subsequent layers. Therefore, other 3D bioprinting techniques have also been used to

produce the multidirectional and interconnected channels. In a recent study, we developed a 3D bio-printed vascularized tissue construct with a unique integration of fully interconnected microvascular networks using a FDM printer (Figure 4d).^[85,129] The microvascular design of the constructs can provide similar flow characteristics to native blood vessels under pulsatile arterial flow.

4.2.1.3. Direct Printing of Tubular Constructs: The third approach is direct bioprinting of blood vessels or vascular networks in a tubular shape via: (1) bioprinting of tubular grafts or vasculature; and (2) bioprinting of scaffold-free branched vascular tubes that are printed inside a mold pattern. Compared to other fabrication methods, direct printing of the self-supporting tubular constructs allows them to be integrated within a multiple bioprinting platform and also facilitates patterning them into complex spatial structures.

Recently, a biodegradable, 3D-printed, acellular vascular graft was fabricated with poly(propylene fumarate) (PPF) using a DLP based SLA technique (Figure 4e).^[130] Both in vitro and in vivo studies showed that this graft-fabrication strategy enabled the printing of scaffolds with inner diameters of 1 mm and wall thicknesses of 150 μm , which sustained patency and functionality for 6 months after implantation in the venous system of mice.^[130] Moreover, our group also developed a complex vascularized tissue construct using a dual 3D bioprinting technique based on the FDM and SLA bioprinter systems.^[87] A biomimetic vascular lumen with capillaries was successfully generated in our engineered construct after the encapsulation of endothelial cells (Figure 4f).^[87]

In one paradigm for direct extrusion of tubular structures, coaxial extrusion nozzles are employed to produce free-standing fluidic channels. The outer nozzle contains an uncrosslinked biopolymer, while the inner nozzle contains the corresponding crosslinker. The freestanding tubular constructs are generated along with the crosslinking process. Typically, the combination of alginate and calcium chloride (CaCl_2) are widely used in 3D printed blood vessels.^[131,132] The stacks of self-standing fibers are printed using a shell/core nozzle through the continuous extrusion of highly concentrated alginate (16.7% w/w) with PVA (6% w/v) solution.^[133] After printing, constructs are transferred to a CaCl_2 solution and the hollow fibers are generated by the dissolution of the PVA.^[133] Furthermore, the low concentrated, cell-laden sodium alginate (2~6%) has been utilized to fabricate hollow tubes without any supports.^[131,134] In this design, the sodium alginate solution flowing through the outer tube of a coaxial nozzle is immediately crosslinked by a CaCl_2 solution through the inner tube.^[134] Although, the coaxial nozzle system offers a very straightforward approach for direct extrusion of tubular structures, this printing method cannot currently achieve branched structures.

The alginate/ CaCl_2 system has also been applied to inkjet printing.^[45] Microgel beads were formed by diffusion of Ca^{2+} into alginate ink droplets by laminating printing to fabricate tubular structures.^[47] The wall thickness and the inner diameters of the tubular structures could be adjusted respectively from 35 to 40 μm and from 30 to 200 μm through varying the diameter of the microgel beads.^[47] In addition, a 3D zigzag tube structure was printed via an inkjet-printing process.^[135] By refining the operating conditions, 210 layers of Ca-alginate

droplets were deposited to form a freestanding tube with a height of 10 mm, an overhang angle of 63° and an overhang height of 5 mm.^[135]

Alginate has shown promising advantages for fabrication of blood vessels, however, it is not an ideal material for living tissue construction.^[50,96,97,136] First, it does not promote cell adhesion due to its strongly hydrophilic nature, thus ECs cannot grow around the tubular construct to form the endothelium layer. Second, the encapsulated cells have limited proliferation due to a lack of natural ECM receptors. Finally, the alginate/CaCl₂ hydrogel is unstable for a long culture time because of its ionic interaction, owing to the exchange reaction with other ions. Therefore, the use of more biomimetic materials instead of, or along with, alginate gel is required. In a different design, coaxial extrusion was used to create a grid of solid alginate/GelMA fibers by extruding an alginate/GelMA mixture through an inner nozzle and calcium chloride through an outer nozzle (Figure 4g).^[136] After a temporary solidification by physical crosslinking, GelMA was covalently photocrosslinked to further reinforce the fibers. Over the culture period, the ionically crosslinked alginate disintegrated leaving hollow, interconnected fluidic channels in the constructs. The results showed ECs encapsulated in the fibers could migrate to the edges of the fibers for endothelium formation. This technique addressed the questions of the instability and weak bioactivity of alginate gels, but it did not provide a biomimetic, hollow, vascular structure. Subsequently, they modified the design to fabricate perfusable hollow tubes using a blended bioink and alginate removal process.^[137]

Combining direct extrusion and a supporting slurry of hydrogel microparticles was also developed. This approach can print hierarchically branching tubular networks. Photoreactive poly(vinyl alcohol) (PVA) was crosslinked after printing and fully crosslinked structures were recovered from the slurry of Carbopol particles by immersion in stirred water.^[138] Concentrically nested objects were also printed, highlighting the potential for this technique to produce biological structures with heterogeneous internal structure.^[138] In another study, gelatin hydrogel microparticles were used with freeform reversible embedding of suspended hydrogels (FRESH) as a support bath to print embedded branching arterial tree.^[139]

Combination of high-resolution TPP with SLA enables the fabrication of refined and complex geometries for printing tubular blood vessels. The tubular or bifurcated structures were created using photo-crosslinkable synthetic polymers and biopolymers. The high resolution of TPP enabled the fabrication of branched tube structures with 18 μm luminal diameter and wall thicknesses <5 μm, using a polytetrahydrofuranetherdiacrylate (PTHF-diacrylate).^[140] The presented artificial vascular constructs possessed 3D microstructured wall architectures, including high porosity and high interconnectivity.^[140] In order to obtain a proper mechanical strength, dithiol-mediated chain transfer was also applied to photo-crosslinkable materials.^[141] The printed networks showed the reduced cross-linking density and high contents of reversible H-bonds, generating the biomimetic mechanical properties in the range of native porcine carotid arteries.^[141]

Scaffold-free bioprinting provides an alternative method based on cells and the genuine matrix they secrete while avoiding the complexity of biomaterials such as biocompatibility, degradation behavior or potential immunogenicity.^[135,142] The extrusion of cell aggregates

consisting of either one cell type or several cell types was developed for the fabrication of tubular structures. A fully biological self-assembly approach was proposed to fabricate the scaffold-free, small diameter, vascular reconstructions.^[143] Various vascular cell types, including SMCs and fibroblasts, were aggregated into discrete units of either multicellular spheroids or cylinders of controllable diameter. Then they were printed by molding a sacrificial template of collagen or agarose.^[143,144] After removing the template, the fusion of the discrete units resulted in single- and double-layered hollow vascular tubes. Unique advantages of this method are speed and scalability; it is capable of engineering blood vessels with distinct shapes/diameters and hierarchical structure.^[143,144]

Although numerous 3D bioprinting approaches have emerged to fabricate the vasculature, generating vasculature with multi-scale, multilayer structures that replicate the geometry, complexity, and longevity of human vascularized tissues remains a challenge. In addition to fabricating the vasculature within the construct, the functionality and anastomosis of in vivo microcirculation should be taken into account for implantation. On one hand, a strategy combining 3D printing and site-specific delivery of angiogenic factors should be developed to promote vascularization. Several studies have shown a positive effect on angiogenesis in our works.^[85,87] On the other hand, the design and bioprinting of vascular networks should be easily connected to native blood vessels, thus it should possess certain properties, such as proper mechanical properties (elasticity and tensile strength) to satisfy retention and burst pressure, sufficient interconnectedness of endothelium to prevent thrombosis, and a high patency rate to support occlusion-free circulation. Compared with indirect bioprinting of a vascular network, the direct bioprinting of tubular construct can be more convenient for anastomosis to the host.

4.2.2. Neural Networks—The human nervous system is widely distributed throughout the body, which is similar with the aforementioned vasculature. It is responsible for controlling all the biological processes that coordinate voluntary and involuntary actions as well as transmit signals among the different parts of the body.^[145] It consists of the central nervous system (CNS) and the peripheral nervous system (PNS).^[145] The CNS consists of the brain and spinal cord and is responsible for processing the information from the PNS.^[146–148] The PNS consists of nerve fiber (Schwann cells (SCs) wrap around the axons) bundles and connective tissues that detect and transmit signals between the CNS and limbs/peripheral organs through motor (or efferent) and sensory (or afferent) nerves.^[149–151] At the cellular level, neurons are the core components of both the CNS and the PNS, which connect to each other to form neural circuits or neural networks.^[145] Based on biological viewpoints, the primary function of the nervous system is to control the whole body via connecting the brain to all tissues/organs. Therefore, the fabrication of neural networks is an essential process for complex tissue and organ regeneration.

Prior to creating neural networks, the repair of nervous system injuries caused by disease, trauma and disorders remains a formidable task.^[146,150] In our previous review and book, we have discussed the self-repair process of the nervous system in detail.^[152,153] Following the PNS injuries, Wallerian degeneration commonly occurs, and SCs are activated to contribute to forming the bands of Büngner, enabling guided axonal regeneration. However, the reconstruction process cannot take place in CNS injuries because the CNS lacks SCs.

Instead, glial scar tissue forms, impeding both axon growth and myelination.^[152] Therefore, tissue engineering techniques combining cells and scaffolds is the most feasible approach for CNS regeneration.^[147,152,154] Although the PNS has a greater capacity for axonal regeneration after injury, spontaneous peripheral nerve repair is nearly always incomplete with poor functional recovery.^[149,150] Misdirection towards the wrong target reduces functional outcome, thus grafts between the nerve stumps are required to bridge the gap and support axonal regrowth. Additionally, the PNS shows poor self-repair ability in large defects. Utilization of an autograft in clinical treatments inevitably creates additional nerve injury and loss of function near the donor site; allografts techniques often induce immunological rejection. To overcome these disadvantages, current research is focused on the development of novel tissue engineering alternatives to repair peripheral nerve gaps.^[150,151]

Overall, nervous system regeneration involves the surgical implantation of a neural scaffold or conduit fabricated in vitro at the targeted site. The scaffold or conduit bridges the lesion, provides a direct framework for neurons to proliferate and promotes cell secretion of inductive factors for axonal elongation and for minimal scar formation.^[145,152] In the human body, neural cells reside within a 3D ECM with micro/nano architecture and spatiotemporal chemical and physical cues. Conventional scaffold or conduit fabrication techniques offer limited control over geometry and internal microstructure, especially for the oriented feature. 3D printing techniques offer great precision and control of the internal architecture and outer shape of the conduits and even have great potential for replicating the complicated nervous network.^[34,152,153,155]

4.2.2.1. 3D Printing for PNS Regeneration: Inkjet bioprinting has shown great potential for fabricating conduits for engineered neural tissue. In an earlier study, the controlled patterns and structures of primary embryonic hippocampal and cortical neurons were first fabricated using a thermal inkjet printer.^[156] The results showed cellular properties and functional fidelity of neurons, including neuronal phenotypes, and electrophysiology could be retained after bioprinting.^[156] Furthermore, a novel bioink based on a microgel suspension (endotoxin-free low-acyl gellan gum) in a surfactant-containing tissue culture medium was used to print neuron-like PC-12 cells using two different commercially available inkjet bioprinting systems.^[157] The bioink performed very well in preventing cell aggregation and promoting cellular differentiation which was confirmed by immunostaining studies.^[157] The LIFT technique has also been utilized to print constructs for neural tissue engineering.^[158] Schwann cells and astroglial cells can survive, proliferate and differentiate well after printing.^[158] In 3D printing, SLA is the most typical technique to create geometrically patterned constructs with high resolution, creating highly aligned nano/micro structures that mimic natural ECM and facilitate the outgrowth of neurites. Glycidyl methacrylate modified hyaluronic acid (GMHA) was printed as scaffolds with different geometries, including hexagonal and circular patterns with different numbers of channels.^[159] The authors proposed that successful fabrication of conduits with multiple channels parallel to the long axis of the lumen could mimic nerve fascicles and the branched scaffolds can mimic a nerve plexus.^[159] Gradients of molecules were patterned along the length of channels during printing and it was hypothesized that such gradients could be

useful in printed nerve guidance conduits.^[159] More over, a dual hydrogel approach was developed for a patterned conduit, where PEG hydrogel served as a cell-restrictive region supplying structure and a cell-permissive, self-assembling gel (Puramatrix or agarose) was made to encapsulate the embryonic dorsal root ganglia (DRG).^[160] A multilayered, on-demand 3D collagen construction with astrocytes and neurons was printed into single-layer and multilayer constructs using a bio-printer with 4-channel dispenser.^[161] The immunostaining suggested the patterned neurons showed neurite outgrowth and neural connectivity in three dimensions.^[161] Nerve guidance conduits (NGCs) with ~50 mm resolution from photocurable poly(ethylene glycol) resin was printed using μ SL technique.^[162] The photocurable form of PEG was permissive for neuronal growth and experimental differentiation in vitro. The conduits had acceptable handling properties and performed comparatively with an autograft control in a thy-1-YFP-H mouse (the YFP+ transgenic mouse strain possesses a population of fluorescently labelled peripheral axons) 3 mm gap injury model after 21 days, with the number of unique axons at the distal end in each repair group being similar (Figure 5a).^[162]

The stem cell replacement has attracted much attention as a promising therapeutic option for neural tissue regeneration, especially for CNS regeneration.^[163] To support the physiological function of stem cells in the implanted tissue site, the use of 3D printed scaffolds that mimic the biologically functional and organizational complexity of the tissue has been regarded as an important approach.^[152,163] In addition, stem cells can secrete various cytokines and growth factors that generate a variety of beneficial effects such as anti-inflammation, neural cell protection, and induction of the endogenic recovery systems.^[153,163] The micro-well/channel arrays as topographic network patterns were made by SLA to guide the growth and differentiation of embryonic stem cells (ESCs) and MSCs towards a neurogenic lineage.^[164] Extrusion-based bioprinting was employed to fabricate scaffold-free conduits using MSC and ESC cylinders.^[165] The multicellular cylindrical units of MSCs and ESCs were prepared and extruded into molded wells made by agarose rods. After the removal of the agarose rods, the fused construct resulted in three hollow channels forming a fully cellular conduit graft.^[165] Compared with autologous graft and commercial collagen conduit graft, the bioprinted graft performed at a comparable level on the sciatic nerve defect model. Both motor and sensory functions exhibited recovery even though limited axon growth was observed.^[165] The indirect 3D printing technique has been developed to fabricate customized conduit molds. A bio-conduit consisting of adipose-derived stem cell (ASC) laden cryopolymerized gelatin methacryloyl (cryoGelMA) gel was prepared for PNS regeneration 3D printing (Figure 5b).^[166] The conduits were fabricated with different geometries using 3D-printed “lock and key” molds, such as the designed multi-channel or bifurcating models and personalized structures. The in vitro result showed cryoGelMA scaffolds supported the attachment, proliferation and survival of the seeded ASCs, and up-regulated the expression of their neurotrophic factors. After implantation in a rat model, the bio-conduit was capable of supporting re-innervation across a 10 mm sciatic nerve gap, with results close to that of autografts in terms of functional and histological assessment.^[166]

Conductive nanobiomaterials have been shown to improve axon outgrowth and enhance connection between artificial substitutes and target injured nerve tissue.^[152,153] They can

assist to stimulate and control neuron activities under electrical stimulation and more effectively guide neural tissue repair. A 3D printable graphene (3DG) composite liquid ink consisting most of graphene with small amounts of polylactide-co-glycolide, was utilized to create neural constructs via extrusion-based 3D printing (Figure 5c).^[167] The resulting 3DG material is mechanically robust and flexible with electrical conductivities greater than 800 S/m. In vitro experiments, in the absence of neurogenic stimuli, reveal that 3DG supports MSC proliferation and neurogenic differentiation. This coincides with hMSCs adopting highly elongated morphologies with features similar to axons and presynaptic terminals. In vivo experiments using a human cadaver nerve model illustrate that 3DG has exceptional handling characteristics and can be intraoperatively manipulated.^[167]

Neurotrophic factors are endogenous molecules critical to the maintenance, survival, proliferation and differentiation of various neuronal populations.^[151–153] They have been used in neural tissue engineering to promote axonal regeneration, neuronal plasticity and neurogenesis. In a study, murine neural stem cells (C17.2), collagen hydrogel, and vascular endothelial growth factor (VEGF)-releasing fibrin gel were printed to construct an artificial neural tissue.^[168] Compared to the control samples (fibrin without the VEGF or VEGF printed directly in collagen), the printed C17.2 cells in the collagen hydrogel showed high viability, and migrated toward the fibrin gel with a total distance of $102.4 \pm 76.1 \mu\text{m}$ over 3 days due to the VEGF induction.^[168] Recently, an imaging-coupled 3D printing approach was developed, facilitating customized neuroregeneration in previously inaccessible ways.^[169] The custom scaffolds were fabricated via a microextrusion printing system. The bifurcating pathways were augmented with 3D printed biomimetic physical cues and path-specific biochemical cues (nerve growth factor, NGF and glial cell line-derived neurotrophic factor, GDNF).^[169] In vitro studies revealed that 3D printed physical and biochemical cues provide axonal guidance and chemottractant/chemokinetic functionality. In vivo studies examining the regeneration of bifurcated injuries across a 10 mm complex nerve gap in rats showed that the 3D printed scaffolds achieved successful regeneration of complex nerve injuries, resulting in enhanced functional return of the regenerated nerve 3D printing (Figure 5d).^[169] Our group also developed a novel 3D patterned scaffold, which has tunable porous structure and embedded core-shell nanoparticles with sustained neurogenic factor (NGF) delivery, using SLA printing and co-axial electro-spraying techniques.^[170] The printed scaffold with nerve growth factor (NGF) nanoparticles greatly increased the length of neurites and directed neurite extension of PC-12 cells along the fiber. In addition, the 3D printed nanocomposite scaffolds also improved the average neurite length of primary cortical neurons 3D printing.^[170]

4.2.2.2. 3D Printing for CNS Regeneration: In a study, piezoelectric inkjet printing was used to print two types of adult rat CNS cells, retinal ganglion cell (RGC) neurons and retinal glia.^[171] The printing process did not effect RGC/glial survival and RGC neurite outgrowth itself. Moreover, the printed glial cells could retain their growth promoting properties.^[171] In another study, 3D brain-like structures were printed using a bio-ink consisting of a novel peptide-modified biopolymer, (arginine-glycineaspartic acid)-gellan gum (RGD-GG), combined with primary cortical neurons 3D printing.^[172] The results demonstrated successful encapsulation, survival and networking of primary cortical neurons

and glial cells in 3D printed RGD-GG modified hydrogels, indicating that cortical neurons responded better to the RGD peptide in RGD-coupled GG than to purified GG.^[172]

In a recent study, two thermoresponsive water-based biodegradable polyurethane dispersions were synthesized for use on self-developed FDM equipment.^[173] The 3D printed neural stem cell (NSC)-laden construct was implanted into a brain injury model of adult zebrafish. The results showed the 3D construct promoted the repair of damaged CNS and rescued the function of impaired nervous systems.^[173] Most recently, a novel 3D neural mini-tissue construct (nMTC) was fabricated by microextrusion bioprinting.^[174] Frontal cortical human NSCs were used for in situ differentiation toward functional neurons and supporting neuroglia. The bioink was comprised of alginate, carboxymethylchitosan (CMC), and agarose, which form a gel by chemical cross-linking following extrusion with hNSC encapsulation.^[174] The results showed that the differentiation of hNSCs resulted in GABAergic neurons, together with glial cells expressing astrocyte and oligodendrocyte lineage markers. Moreover, the neurons are spontaneously active and show a bicuculline-induced increased calcium response.^[174]

As we discussed above, 3D printing has the capacity to rapidly fabricate subtle exterior geometries as well as complex interior microarchitectures. Therefore, 3D printing has shown its huge potential for neural tissue regeneration. Although most research currently focuses on neural regeneration with the purpose of repairing the nervous system, we believe its success would also pave the way for regenerating neural networks for engineered complex tissues/organs.

4.2.3. Organs—Due to the shortage of organs suitable for transplantation, researchers are now exploring development of functional, full-sized organs using tissue engineering technology. 3D bioprinting holds great promise for achieving all goals, but whole-organ bioprinting, incorporating all of these components has remained elusive largely due to organ-level complexities.^[20,23,26,35,110,175] Therefore, current research in the 3D printed organ field focuses on the biomimetic fabrication of vascularized tissue and their functionalization. In biology, an organ is a collection of tissues joined in a structural unit to serve a common function, including sensory organ, visceral organ, and others.^[1–3] Herein, we mainly focus on visceral organs (internal organs), such as the heart and liver, due to the unique challenges in replicating their highly complex structures and functions.

4.2.3.1. Heart: The heart is a muscular organ in humans, which pumps blood throughout the body in the circulatory system.^[110,176] During embryonic development, the heart is the first functional organ to be developed from the splanchnopleuric mesenchyme cell layer. In anatomy, the heart has four chambers, four valves and a heart wall. The heart valves ensure unidirectional flow of blood: the atrioventricular/inflow valves (mitral and tricuspid) and the semilunar/outflow valves (aortic and pulmonary).^[176] Each valve is composed of leaflets and a fibrous annulus wall (root wall). Leaflets and root walls mainly contain valve interstitial cells (VIC) and smooth muscle cells (SMC) respectively, with valvular endothelial cells (VEC) covering on the surface.^[176] The heart wall is made up of three layers: the inner endocardium, middle myocardium and outer epicardium/pericardium.^[176] The endocardium is primarily made up of endothelial cells, which act as a blood–heart

barrier to protect the valves and heart chambers. The myocardium consisting of cardiomyocytes is the thick muscular layer responsible for contraction and relaxation of the heart. The pericardium is a double-wall fibroserous sac that acts to protect the heart, anchoring it to the surrounding walls, and preventing it from overfilling with blood.^[176] Overall, the heart includes three main cellular components, cardiomyocytes, fibroblasts, and endothelial cells. In the treatment of serious cardiovascular disease (CVD), traditional approaches, including autografts, allografts, xenografts, and artificial prostheses, have several disadvantages, such as donor tissue shortage, immune rejection, anticoagulation therapy, and limited durability. Tissue engineering techniques have shown a promising approach for creating engineered tissues to repair congenital defects and/or diseased cardiovascular tissues. 3D bioprinting has recently been an efficient approach to reproduce the complexity of structural and functional cardiac tissues.^[110]

The most fatal CVD is myocardial infarction (MI), caused by the blockage of the coronary arteries. Myocardial ischemia sets off a series of complicated and irreversible processes, involving cell death, scar formation, and ventricular dysfunction.^[177] Therefore, engineered myocardial tissue has been explored to restore cardiac functions using 3D printing techniques. LIFT-based cell printing techniques were first applied to prepare a polyester urethane urea (PEUU) cardiac patch seeded with HUVECs and MSCs in a defined pattern for cardiac regeneration.^[178] Compared with the random patch, the patterned patch showed increased vessel formation and found significant functional improvement of infarcted hearts following implantation.^[178] Human cardiac derived cardiomyocyte progenitor cell (hCMPC)-laden alginate hydrogel was used to print the 3D cardiac construct.^[179] The printed construct retained the cardiac phenotype with high cell viability. Moreover, the 3D culture enhanced gene expression of the early cardiac transcription factors Nkx2.5, Gata-4 and Mef-2c as well as the sarcomeric protein TroponinT.^[179]

Dysfunctional valves caused by stenosis or regurgitation impair the proper opening and closing of the valves, affecting efficient heart performance.^[110] Compared with traditional approaches, tissue engineering has great potential to address current limitations of non-living prosthetics by providing living constructs that can grow, remodel and integrate in patients. For the engineered heart valve, 3D bioprinting can create anatomically accurate, living, engineered valves with heterogeneous mechanical properties and well-distributed multiple cells. In an earlier study, native anatomic and axisymmetric aortic valve geometries (root wall and trileaflets) with 12–22 mm inner diameters were 3D printed with a dual-nozzle printer.^[180] PEG-DA hydrogels and alginate hydrogels were utilized to fabricate the heterogeneous aortic valve constructs with different mechanical properties. VIC seeded scaffolds maintained near 100% viability over 21 days.^[180] In addition, a 3D simplified heart valve construct with root and trileaflets was printed from a HAMA/GelMA based hybrid hydrogel.^[181] Human aortic VICs were encapsulated into the bioprinted hydrogel, which maintained high viability, and remodeled the initial matrix by depositing collagen and glycosaminoglycans.^[181] They also used alginate/gelatin hydrogel to bioprint a living 3D heart valve with anatomical architecture (Figure 6a).^[182] Direct encapsulation of aortic root sinus SMCs in the valve root and aortic VICs in the leaflet were viable ($81.4 \pm 3.4\%$ for SMCs and $83.2 \pm 4.0\%$ for VICs) over 7 days in culture. Moreover, the encapsulated SMCs

expressed higher alpha-smooth muscle actin (α -SMA) in the printed stiff matrix, while the soft matrix elevated vimentin expression of the VICs.^[182]

Some researchers have developed bioprinted cardiac and valve constructs for cardiac and valve tissue engineering, but a functional 3D heart construct has yet to be explored. The whole heart organ not only has complicated structure, but is also comprised of multiple cell types with spatial distribution, associating with specific and integrated functions comparable to native tissue. Recently, the FRESH technique has also been developed to create a 3D heart construct of a 5-day-old chick embryo, demonstrating the capability of recapitulating the complex trabecular structures of a whole heart through CAD modeling (Figure 6b).^[139] Although it is still not a functional heart with a vascular network, it offers a potential approach to generate a large-scale, complex 3D internal and external anatomical architecture.

4.2.3.2. Liver: In the human body, the liver is composed of highly specialized tissue consisting of mostly hepatocytes. It plays a major role in metabolism with numerous functions, including regulation of glycogen storage, decomposition of red blood cells, plasma protein synthesis, hormone production, and detoxification.^[1,176] In anatomy, the liver is divided into four lobes, each of which is microscopically made up of hepatic lobules. The lobules are roughly hexagonal, and consist of hepatocyte plates radiating from a central vein.^[176] Between the hepatocyte plates are liver sinusoids, which connect the central vein with the portal triads for mixing of the oxygen-rich blood from the hepatic artery and the nutrient-rich blood from the portal vein.^[176] Histology shows two major types of liver cell: parenchymal cells and non-parenchymal cells. The parenchymal cells are hepatocytes that constitute 70~85% of the liver volume. The non-parenchymal cells are sinusoidal endothelial cells (SECs), phagocytic Kupffer cell (KCs), and hepatic stellate cells (HSCs), among others. Owing to its location and multidimensional functions, the liver is also prone to many diseases.^[176]

The liver has extensive regeneration capacity due to high proliferation ability of hepatocytes, even if it is subjected to vast damages. Therefore, various tissue engineering techniques have been developed to fabricate biomimetic liver tissues. However, the traditional methods have a limited achievement on the volumetric liver tissues with highly intercellular adhesion.^[183] 3D bioprinting facilitates the fabrication of complex liver structures with higher cell densities.^[110]

In an earlier work, a 3D hepatocyte/gelatin construct was printed from a 38 layer assembly.^[184] The laminated hepatocytes remained viable and performed biological functions in the construct for more than 2 months. This technique showed a promising and stepwise approach to reconstitute the structure of the in vivo microenvironment of human livers.^[184] Some researchers also focus on fabricating micro-organs or organs-on-a-chip using 3D printing for drug metabolic studies.^[110] A multi-nozzle extrusion system was applied to fabricate human liver hepatocellular carcinoma cell (HepG2) laden alginate hydrogel in an organized 3D architecture.^[185] The biofabricated micro-organ device was performed as an in vitro drug metabolism model. The results showed a biomimetic drug metabolic process in the micro-organ under continuous perfusion flow.^[185] In another study,

a liver-on-a-chip platform of 3D human HepG2/C3A spheroids was also developed for drug toxicity assessment.^[186] The engineered bioreactor could be interfaced with a bioprinter to fabricate 3D hepatic spheroids encapsulated within GelMA hydrogel. The engineered hepatic constructs remained functional for 30 days while monitoring the secretion rates of albumin, alpha-1 antitrypsin, transferrin, and ceruloplasmin, as well as immunostaining for the hepatocyte markers, cytokeratin 18, MRP2 bile canalicular protein and tight junction protein ZO-1.^[186] In addition, an acetaminophen-induced toxic response test in this platform was performed to verify the effectiveness similar to that of animal studies.^[186]

Recently, metabolically active, anatomical, 3D hepatic tissues have also been developed. For example, a double-nozzle bioprinting technique was used to fabricate an anatomical liver structure with a vascular-like network.^[187] Adipose-derived stromal cells (ADSCs) were encapsulated within a gelatin/alginate/fibrinogen hydrogel to form a vascular-like network, and hepatocytes laden gelatin/alginate/chitosan hydrogel was placed around it. The ADSCs were induced to differentiate into endothelial-like cells with endothelial growth factor. The albumin secretion level of the embedded hepatocytes increased during the 2 week culture, while the levels of urea and alanine transaminase were decreased after an increasing profile. These results indicate that this double-nozzle assembly technique could be a powerful tool for fabricating complex liver constructs with special intrinsic/extrinsic structures.^[187] Using NovoGen™ bio-printing technology (Organovo Holdings, Inc., San Diego, CA, USA), 3D liver constructs were fabricated containing architecturally and physiologically relevant features for two hepatic cell lines and primary hepatocytes.^[188,189] Bioprinted 3D hepatic neotissues were further enhanced in complexity with the addition of ECs and HSCs. Biochemical studies demonstrated that several critical liver functions were present, and tight junction protein expression was observed throughout the 3D tissue. Moreover, the 3D printed liver tissues also underwent other biochemical studies for six weeks. In addition to the liver-specific functions, it also exhibited a clinically relevant injury response. These results demonstrate the potential utility of human 3D bioprinted liver tissues in drug discovery and development.^[189] Most recently, a 3D hydrogel-based triculture model that embeds hiPSC-derived hepatic progenitor cells (hiPSC-HPCs) with human umbilical vein endothelial cells and adipose-derived stem cells in a microscale hexagonal architecture was developed using a DLP technique (Figure 6c).^[190] In comparison with 2D monolayer culture and a 3D HPC-only model, the 3D triculture model showed both phenotypic and functional enhancements in the hiPSC-HPCs over weeks of in vitro culture, especially for improved morphological organization, higher liver-specific gene expression levels, increased metabolic product secretion, and enhanced cytochrome P450 induction.^[190]

Overall, although 3D printing of complex and large 3D organs currently remains an arduous challenge, it has shown promising results toward the generation of ‘mini-organs’ that contain the same functional components of large organs.^[191] Mini-organs can be considered a future trend in organ printing and might be a gateway to fully functional organs. They can be built in smaller scale than their natural counterparts while closely performing the most vital function of the associated organ. From the current studies, the simultaneous printing of multiple materials could allow fabrication of engineered tissues with heterogeneous internal organization of cells and ECM, which could more accurately model native tissue organization. Additionally, multiple organ-specific cell types are required to be spatially

organized to form functional organs, especially for the integration of vasculature within the constructs.

5. Current Challenges and Future Perspectives

Organ printing is a multidisciplinary technology including biology, engineering, materialogy, computer science, and medicine, which requires a multidisciplinary team and long-term sustainable financial support. Over the past few years, researchers not only have demonstrated proof-of-concept examples of artificial tissue fabrication using different bioprinting technologies, but also have shown possibilities that 3D bioprinting offers an effective method of recapitulating structural and functional complexity for engineered tissue fabrication, especially for functional organ fabrication. Many of the challenges facing the 3D bioprinting field relate to specific technical, material, and cellular aspects.

Considering the pathway from 3D organ printing to implantation into a human in a reasonable amount of time, standardized protocols involving patient-specific design, fabrication techniques, maturation processes, surgical operations and postoperative care are essential for customized functional organ fabrication. First, considering printing techniques, current 3D tissue/organ printing has to address many technical challenges to increase the resolution, printing speed and flexibility with relevant biomaterials for creating more complex and composite tissue/organ structures at clinically relevant sizes. Secondly, bioinks and cells must be considered. The 3D construct generated by bioprinting serves as a biomimetic construct with desired composition and cellular contribution to support functionality. Moreover, it is unlikely that any single material and single cell possess all the properties required to recapitulate tissue function. Therefore, developing appropriate bioink formulations associating with cell sources with sufficient supply are very important. The third consideration is fabrication strategy. Organs have highly complex architectures and properties; as such they may require a combination of several bioprinting techniques along with specifically designed bioinks to introduce structural heterogeneity and functionality. Highly repeatable and straightforward technologies and protocols should be developed to print the organs in logical steps, from simple to complex. The fourth consideration is the manufacturing process. Considering the micro-scale resolution in cellular bioprinting, the process requires enough nutrients and oxygen supplementation for sustaining scalable living constructs in a stable, sterile printing system over long printing times. The post-bioprinting process is the fifth consideration. Another challenge for organ printing technology is the rapid or accelerated tissue maturation process, where printed organ constructs should undergo rapid matrix deposition, remodeling, and maturation toward a solid living tissue with bioink degradation, ensuring structural integrity, mechanical rigidity and biological functionality for implantation. As an alternative, in situ bioprinting is an advanced trend in organ regeneration, where living cells can be printed in the human body during an operation instead of the post-bioprinting process in vitro.^[26,50] It can enable growth of thick tissues in critical defects with the help of vascularization driven by natural processes in the body. Although in situ bioprinted skin and bone have been tested, the manufacturing of complex organs is still uncertain in view of the limited success of their fabrication in vitro.^[26]

Finally, in order to ensure effective industrial translation and commercialization of organ printing technology, the key issue is quality assurance and regulation of bioinks, bioprinters and bioprinted products. This customizable 3D product requires a comprehensive regulation to assure quality control in every step of the process: production of printing equipment and raw materials (bioprinter, biomaterials, biological factors and cells), design control of the 3D printed model, validation of the manufacturing along with its governing software, product testing and finally the implantation process. The FDA issued draft guidance on May 10, 2016, titled “Technical Considerations for Additive Manufactured Devices”, which provides guidance for manufacturers who are producing devices through 3D printing techniques. In March, the FDA approved Aprexia Pharmaceuticals’ SPRITAM® (levetiracetam), which was the first FDA-approved drug manufactured using 3D printing. In addition to regulation, ethical concerns will be considered for future attempts. Although the majority of the trials have been made on animals, ethical concerns will be raised when printing tissues or organs for implantation in humans.

New niches for technological advancements on instrumentation, with improved spatial and temporal resolutions as well as optimized bioinks and cell sources for specific organs, provide promise that 3D bioprinting will eventually become one of the most efficient, reliable, and convenient methods to biofabricate tissue constructs in the near future. The high flexibility and controllability of 3D bioprinting enables complex and tailored release profiles of multiple active pharmaceuticals with spatiotemporal gradients for regulating cellular functions during tissue/organ regeneration.^[82,192] A unique aspect of this technology is its ability to achieve a personalized therapeutic schedule to address individual patient needs.^[193] Moreover, advanced materials engineering approaches featuring biologically dynamic variations will further allow temporal evolution of bioprinted tissue constructs that potentially meet the requirements of dynamic tissue remodeling during developmental processes. For instance, 4D bioprinting techniques have been proposed,^[27] and our lab has developed some 4D bioprinted constructs for regulating cell/scaffold behavior.^[61,194] Furthermore, 3D bioprinting techniques have shown the potential to facilitate the development of realistic tissue/organ models, therefore this technology is also expected to translate advancing the needs of other specific applications such as models for pharmaceutical/toxicological screening.^[36,195]

6. Conclusion

3D bioprinting for organ regeneration is an emerging field that encompasses specific technical, material and cellular aspects, and is in the initial stages of development. However, this technology has already demonstrated its remarkable potential for future development and 3D scale-up of functional organs; its versatility has also been expanded to other applications, such as in vitro tissue/organ models for various research studies. This review presents the recent advances in the bioprinting and their relative components, including the techniques, the bioinks, the cells, and applications for organ regeneration. Although challenges still remain in this research field, further multidisciplinary research to advance printing techniques, printable bioink materials and engineering designs can address the current challenges and realize the emerging potential of 3D organ bioprinting.

Acknowledgements

This work is supported by NIH Director's New Innovator Award 1DP2EB020549-01, NSF BME program grant # 1510561, NSF MME program grant # 1642186 and March of Dimes Foundation's Gene Discovery and Translational Research Grant.

Biography



Haitao Cui received his Ph.D. in chemistry and physics of polymers in 2015 from Changchun Institute of Applied Chemistry, Chinese Academy of Sciences. He joined the Prof. Zhang's group in March 2015. His research currently focuses on the development of novel biomaterials, 3D bioprinting, and complex tissue/organ regeneration.



Margaret Nowicki is currently completing her PhD in Mechanical Engineering at The George Washington University School of Engineering and Applied Sciences under the supervision of Dr. Lijie Grace Zhang. Her research interests include 3D/4D bioprinting, complex tissue engineering, and nanobiomaterials.



Lijie Grace Zhang is an associate professor in the Department of Mechanical and Aerospace Engineering at the George Washington University. She obtained her Ph.D. in Biomedical Engineering at Brown University in 2009 and did her postdoctoral training at Rice University and Harvard Medical School. She is the director of the Bioengineering Laboratory for Nanomedicine and Tissue Engineering at GW. Her research interests include

3D/4D bioprinting, complex tissue engineering, nanobiomaterials, stem cell engineering, drug delivery and breast cancer bone metastasis.

References

- [1]. Widmaier, EP., Raff, H., Strang, KT. Vander's Human Physiology. McGraw-Hill Education; Boston, NY, USA: 2010.
- [2]. Badyalak SF, Weiss DJ, Caplan A, Macchiarini P. *Lancet*. 2012; 379:943. [PubMed: 22405797]
- [3]. Rustad KC, Sorkin M, Levi B, Longaker MT, Gurtner GC. *Organogenesis*. 2010; 6:151. [PubMed: 21197216]
- [4]. Zhang, LG., Khademhosseini, A., Webster, TJ. *Tissue and Organ Regeneration: Advances in Micro and Nanotechnology*. Pan Stanford Publishing; Stanford: 2014.
- [5] a). Castro NJ, O'Brien CM, Zhang LG. *AIChE J*. 2014; 60:432. b) Zhu W, Masood F, O'Brien J, Zhang LG. *Nanomedicine*. 2015; 11:693. [PubMed: 25596341] c) Cui H, Zhuang X, He C, Wei Y, Chen X. *Acta Biomater*. 2015; 11:183. [PubMed: 25242655] d) Cui HT, Liu YD, Cheng YL, Zhang Z, Zhang PB, Chen XS, Wei Y. *Biomacromolecules*. 2014; 15:1115. [PubMed: 24597966] e) Cui HT, Shao J, Wang Y, Zhang PB, Chen XS, Wei Y. *Biomacromolecules*. 2013; 14:1904. [PubMed: 23611017] f) Cui H, Cui L, Zhang P, Huang Y, Wei Y, Chen X. *Macromol. Biosci*. 2014; 14:440. [PubMed: 24821672]
- [6]. Cui H, Wang Y, Cui L, Zhang P, Wang X, Wei Y, Chen X. *Bio-macromolecules*. 2014; 15:3146.
- [7]. Place ES, Evans ND, Stevens MM. *Nat. Mater*. 2009; 8:457. [PubMed: 19458646]
- [8]. Zhang LJ, Webster TJ. *Nano Today*. 2009; 4:66.
- [9]. Derby B. *Science*. 2012; 338:921. [PubMed: 23161993]
- [10]. Griffith LG, Swartz MA. *Nat. Rev. Mol. Cell Biol*. 2006; 7:211. [PubMed: 16496023]
- [11]. Dvir T, Timko BP, Kohane DS, Langer R. *Nat. Nanotechnol*. 2011; 6:13. [PubMed: 21151110]
- [12]. Benetti EM, Gunnewiek MK, van Blitterswijk CA, Julius Vancso G, Moroni L. *J. Mater. Chem. B*. 2016; 4:4244.
- [13]. Zan G, Wu Q. *Adv. Mater*. 2016; 28:2099. [PubMed: 26729639]
- [14]. Billiet T, Vandehaute M, Schelfhout J, Van Vlierberghe S, Dubruel P. *Biomaterials*. 2012; 33:6020. [PubMed: 22681979]
- [15]. Li J, He L, Zhou C, Zhou Y, Bai Y, Lee FY, Mao JJ. *MRS Bull*. 2015; 40:145.
- [16]. Mandrycky C, Wang Z, Kim K, Kim DH. *Biotechnol. Adv*. 2016; 34:422. [PubMed: 26724184]
- [17]. Ozbolat IT, Yu Y. *IEEE Trans. Biomed. Eng*. 2013; 60:691. [PubMed: 23372076]
- [18]. O'Brien CM, Holmes B, Faucett S, Zhang LG. *Tissue Eng., Part B*. 2015; 21:103.
- [19] a). Farahani RD, Dube M, Therriault D. *Adv. Mater*. 2016; 28:5794. [PubMed: 27135923] b) Kalsoom U, Nesterenko PN, Paull B. *Rsc Adv*. 2016; 6:60355. c) Ambrosi A, Pumera M. *Chem. Soc. Rev*. 2016; 45:2740. [PubMed: 27048921]
- [20]. Murphy SV, Atala A. *Nat. Biotechnol*. 2014; 32:773. [PubMed: 25093879]
- [21]. Do AV, Khorsand B, Geary SM, Salem AK. *Adv. Healthcare Mater*. 2015; 4:1742.
- [22]. Park JH, Jang J, Lee JS, Cho DW. *Ann. Biomed. Eng*. 2016; doi: 10.1007/s10439-016-1611-9
- [23]. Mironov V, Richard VK, Visconti P, Forgacs G, Drake CJ, Markwald RR. *Biomater. Sci*. 2009; 302164
- [24]. Zorlutuna P, Annabi N, Camci-Unal G, Nikkhah M, Cha JM, Nichol JW, Manbachi A, Bae H, Chen S, Khademhosseini A. *Adv. Mater*. 2012; 24:1782. [PubMed: 22410857]
- [25]. Rengier F, Mehndiratta A, von Tengg-Kobligk H, Zechmann CM, Unterhinninghofen R, Kauczor HU, Giesel FL. *Int. J. Comput. Assist. Radiol. Surg*. 2010; 5:335. [PubMed: 20467825]
- [26]. Ozbolat IT. *Trends Biotechnol*. 2015; 33:395. [PubMed: 25978871]
- [27]. Gao B, Yang Q, Zhao X, Jin G, Ma Y, Xu F. *Trends Biotechnol*. 2016; 34:746. [PubMed: 27056447]
- [28]. Hull, CW. *US. 4575330 A*. 1986.

- [29]. Wilson WC Jr, Boland T. *Anat. Rec. A Discov. Mol. Cell. Evol. Biol.* 2003; 272:491. [PubMed: 12740942]
- [30]. Murphy, K., Dorman, S., Smith, N., Bauwens, L., Sohn, I., McDonald, T., Leigh-Lancaster, C., Law, RJ. *US. 20120116 568 A1.* 2012.
- [31]. Jose RR, Rodriguez MJ, Dixon TA, Omenetto F, Kaplan DL. *ACS Biomater. Sci. Eng.* 2016; 2:1662.
- [32]. Food and Drug Administration. *Technical Considerations for Additive Manufactured Devices.* 2016
- [33]. Zhang X, Zhang Y. *Cell Biochem. Biophys.* 2015; 72:777. [PubMed: 25663505]
- [34]. Zhang, LG., Fisher, JP., Leong, KW. *3D Bioprinting and Nanotechnology in Tissue Engineering and Regenerative Medicine.* Elsevier Ltd; San Diego: 2015.
- [35]. Mironov V, Kasyanov V, Markwald RR. *Curr. Opin. Biotechnol.* 2011; 22:667. [PubMed: 21419621]
- [36]. Pati F, Gantelius J, Svahn HA. *Angew. Chem. Int. Ed. Engl.* 2016; 55:4650. [PubMed: 26895542]
- [37]. Gu BK, Choi DJ, Park SJ, Kim MS, Kang CM, Kim CH. *Biomater. Res.* 2016; 20:12. [PubMed: 27114828]
- [38]. Skardal A, Atala A. *Ann. Biomed. Eng.* 2015; 43:730. [PubMed: 25476164]
- [39]. Gasperini L, Maniglio D, Motta A, Migliaresi C. *Tissue Eng., Part C.* 2015; 21:123.
- [40]. Mezel C, Souquet A, Hallo L, Guillemot F. *Biofabrication.* 2010; 2:014103. [PubMed: 20811118]
- [41]. Nishiyama Y, Henmi C, Iwanaga S, Nakagawa H, Yamaguchi K, Akita K, Mochizuki S, Takiura K, Nakamura M. *J. Imaging Sci. Technol.* 2008; 52:60201.
- [42]. Khalil S, Nam J, Sun W. *Rapid Prototyping J.* 2005; 11:9.
- [43] a). Cui X, Boland T, D'Lima DD, Lotz MK. *Recent Pat. Drug Delivery Formul.* 2012; 6:149.b) Tekin E, Smith PJ, Schubert US. *Soft Matter.* 2008; 4:703.
- [44]. Demirci U, Montesano G. *Lab Chip.* 2007; 7:1139. [PubMed: 17713612]
- [45]. Xu T, Zhao W, Zhu JM, Albanna MZ, Yoo JJ, Atala A. *Biomaterials.* 2013; 34:130. [PubMed: 23063369]
- [46]. Eagles PA, Qureshi AN, Jayasinghe SN. *Biochem. J.* 2006; 394:375. [PubMed: 16393140]
- [47]. Nakamura M, Nishiyama Y, Henmi C, Iwanaga S, Nakagawa H, Yamaguchi K, Akita K, Mochizuki S, Takiura K. *J. Imaging Sci. Technol.* 2008; 52:060201.
- [48]. Tao H, Marelli B, Yang M, An B, Onses MS, Rogers JA, Kaplan DL, Omenetto FG. *Adv. Mater.* 2015; 27:4273. [PubMed: 26079217]
- [49]. Jia C, Yu D, Lamarre M, Leopold PL, Teng YD, Wang H. *Adv. Mater.* 2014; 26:8192. [PubMed: 25352221]
- [50]. Ozbolat IT, Hospodiuk M. *Biomaterials.* 2016; 76:321. [PubMed: 26561931]
- [51]. Lewis JA, Gratson GM. *Mater. Today.* 2004; 7:32.
- [52]. Panwar A, Tan LP. *Molecules.* 2016; 21:685.
- [53]. Chang CC, Boland ED, Williams SK, Hoying JB. *J. Biomed. Mater. Res. B Appl. Biomater.* 2011; 98:160. [PubMed: 21504055]
- [54]. Ozbolat IT, Chen H, Yu Y. *Robot. Comput. Integr. Manuf.* 2014; 30:295.
- [55]. Pfister A, Landers R, Laib A, Hubner U, Schmelzeisen R, Mulhaupt R. *J. Polym. Sci., Part A: Polym. Chem.* 2004; 42:624.
- [56]. Landers R, Hubner U, Schmelzeisen R, Mulhaupt R. *Biomaterials.* 2002; 23:4437. [PubMed: 12322962]
- [57]. Skoog SA, Goering PL, Narayan RJ. *J. Mater. Sci. Mater. Med.* 2014; 25:845. [PubMed: 24306145]
- [58]. Stansbury JW, Idacavage MJ. *Dent. Mater.* 2016; 32:54. [PubMed: 26494268]
- [59] a). Odde DJ, Renn MJ. *Biotechnol. Bioeng.* 2000; 67:312. [PubMed: 10620261] b) Zhou X, Castro NJ, Zhu W, Cui H, Aliabouzar M, Sarkar K, Zhang LG. *Sci. Rep.* 2016; 6:32876. [PubMed: 27597635]

- [60]. Zhu W, Wang M, Fu Y, Castro NJ, Fu SW, Zhang LG. *Acta Biomater.* 2015; 14:164. [PubMed: 25528534]
- [61]. Miao S, Zhu W, Castro NJ, Nowicki M, Zhou X, Cui H, Fisher JP, Zhang LG. *Sci. Rep.* 2016; 6:27226. [PubMed: 27251982]
- [62]. Park JH, Hong JM, Ju YM, Jung JW, Kang HW, Lee SJ, Yoo JJ, Kim SW, Kim SH, Cho DW. *Biomaterials.* 2015; 62:106. [PubMed: 26041482]
- [63]. Raman R, Bhaduri B, Mir M, Shkumatov A, Lee MK, Popescu G, Kong H, Bashir R. *Adv. Healthcare Mater.* 2016; 5:610.
- [64]. Jariwala SH, Lewis GS, Bushman ZJ, Adair JH, Donahue HJ. *3D Print. Add. Manufact.* 2015; 2:56.
- [65]. Melchels FPW, Domingos MAN, Klein TJ, Malda J, Bartolo PJ, Hutmacher DW. *Prog. Polym. Sci.* 2012; 37:1079.
- [66]. Holmes B, Zhu W, Li J, Lee JD, Zhang LG. *Tissue Eng., Part A.* 2015; 21:403. [PubMed: 25088966]
- [67]. Davidson JR, Appuhamillage GA, Thompson CM, Voit W, Smaldone RA. *ACS Appl. Mater. Interfaces.* 2016; 8:16961. [PubMed: 27299858]
- [68]. Yap CY, Chua CK, Dong ZL, Liu ZH, Zhang DQ, Loh LE, Sing SL. *Appl. Phys. Rev.* 2015; 2:041101.
- [69]. Zhang LC, Attar H, Calin M, Eckert J. *Mater. Technol.* 2016; 31:66.
- [70]. Tumbleston JR, Shirvanyants D, Ermoshkin N, Januszewicz R, Johnson AR, Kelly D, Chen K, Pinschmidt R, Rolland JP, Ermoshkin A, Samulski ET, DeSimone JM. *Science.* 2015; 347:1349. [PubMed: 25780246]
- [71]. Vorndran E, Klarner M, Klammert U, Grover LM, Patel S, Barralet JE, Gbureck U. *Adv. Eng. Mater.* 2008; 10:B67.
- [72]. Birkholz MN, Agrawal G, Bergmann C, Schroder R, Lechner SJ, Pich A, Fischer H. *Biomed. Eng.-Biomed. Tech.* 2016; 61:267.
- [73]. Brunello G, Sivoletta S, Meneghello R, Ferroni L, Gardin C, Piattelli A, Zavan B, Bressan E. *Biotechnol. Adv.* 2016; 34:740. [PubMed: 27086202]
- [74]. Castilho M, Moseke C, Ewald A, Gbureck U, Groll J, Pires I, Tessmar J, Vorndran E. *Biofabrication.* 2014; 6:12.
- [75]. Lee JW. *J. Nanomater.* 2015; 2015:1.
- [76]. Xing JF, Zheng ML, Duan XM. *Chem. Soc. Rev.* 2015; 44:5031. [PubMed: 25992492]
- [77] a). Guvendiren M, Molde J, Soares RMD, Kohn J. *ACS Biomater. Sci. Eng.* 2016; 2:1679. [PubMed: 28025653] b) Hofmann M. *ACS Macro Lett.* 2014; 3:382.
- [78]. Li X, Cui R, Sun L, Aifantis KE, Fan Y, Feng Q, Cui F, Watari F. *Int. J. Polym. Sci.* 2014; 2014:1.
- [79]. Chia HN, Wu BM. *J. Biol. Eng.* 2015; 9:4. [PubMed: 25866560]
- [80]. Zhu W, Ma X, Gou M, Mei D, Zhang K, Chen S. *Curr. Opin. Biotechnol.* 2016; 40:103. [PubMed: 27043763]
- [81]. Lei M, Wang X. *Molecules.* 2016; 21:539.
- [82]. Park JY, Shim J-H, Choi S-A, Jang J, Kim M, Lee SH, Cho D-W. *J. Mater. Chem. B.* 2015; 3:5415.
- [83] a). Mitchell AC, Briquez PS, Hubbell JA, Cochran JR. *Acta Biomater.* 2016; 30:1. [PubMed: 26555377] b) Ahadian S, Sadeghian RB, Salehi S, Ostrovidov S, Bae H, Ramalingam M, Khademhosseini A. *Bioconjugate Chem.* 2015; 26:1984.
- [84]. Tang Z, Wang Y, Podsiadlo P, Kotov NA. *Adv. Mater.* 2006; 18:3203.
- [85]. Cui H, Zhu W, Holmes B, Zhang LG. *Adv. Sci.* 2016; 3:1600058.
- [86]. Lee SJ, Lee D, Yoon TR, Kim HK, Jo HH, Park JS, Lee JH, Kim WD, Kwon IK, Park SA. *Acta Biomater.* 2016; 40:182. [PubMed: 26868173]
- [87]. Cui H, Zhu W, Nowicki M, Zhou X, Khademhosseini A, Zhang LG. *Adv. Healthcare Mater.* 2016; 5:2174.

- [88] a). Wu YL, Putcha N, Ng KW, Leong DT, Lim CT, Loo SC, Chen X. *Acc. Chem. Res.* 2013; 46:782. [PubMed: 23194178] b) Shin SR, Aghaei-Ghareh-Bolagh B, Gao X, Nikkhah M, Jung SM, Dolatshahi-Pirouz A, Kim SB, Kim SM, Dokmeci MR, Tang XS, Khademhosseini A. *Adv. Funct. Mater.* 2014; 24:6136. [PubMed: 25419209] c) Gribova V, Auzely Velly R, Picart C. *Chem. Mater.* 2012; 24:854. [PubMed: 25076811] d) Costa RR, Mano JF. *Chem. Soc. Rev.* 2014; 43:3453. [PubMed: 24549278] e) Hung KC, Tseng CS, Dai LG, Hsu SH. *Biomaterials.* 2016; 83:156. [PubMed: 26774563]
- [89] a). Tarafder S, Koch A, Jun Y, Chou C, Awadallah MR, Lee CH. *Biofabrication.* 2016; 8:025003. [PubMed: 27108484] b) Legemate K, Tarafder S, Jun Y, Lee CH. *J. Dent. Res.* 2016; 95:800. [PubMed: 27053116] c) Shim JH, Kim SE, Park JY, Kundu J, Kim SW, Kang SS, Cho DW. *Tissue Eng. Part A.* 2014; 20:1980. [PubMed: 24517081]
- [90]. Zheng YF, Gu XN, Witte F. *Mater. Sci. Eng. R-Rep.* 2014; 77:1.
- [91]. Li XM, Gao MJ, Jiang Y. *Ceram. Int.* 2016; 42:12531.
- [92]. Bourzac K. *Technol. Rev.* 2016; 119:92.
- [93] a). Goncalves EM, Oliveira FJ, Silva RF, Neto MA, Fernandes MH, Amaral M, Vallet-Regi M, Vila M. *J. Biomed. Mater. Res. Part B.* 2016; 104:1210. b) Kumar A, Nune KC, Misra RDK. *J. Biomed. Mater. Res. Part A.* 2016; 104:1343. c) Wang Q, Xia QQ, Wu Y, Zhang XL, Wen FQ, Chen XW, Zhang SF, Heng BC, He Y, Ouyang HW. *Adv. Healthcare Mater.* 2015; 4:1701.
- [94]. Jungst T, Smolan W, Schacht K, Scheibel T, Groll J. *Chem. Rev.* 2016; 116:1496. [PubMed: 26492834]
- [95]. Wu W, DeConinck A, Lewis JA. *Adv. Mater.* 2011; 23:H178. [PubMed: 21438034]
- [96]. Lee KY, Mooney DJ. *Prog. Polym. Sci.* 2012; 37:106. [PubMed: 22125349]
- [97]. Giri TK, Thakur D, Alexander A, Ajazuddin, Badwaik H, Tripathi DK. *Curr. Drug Delivery.* 2012; 9:539.
- [98]. Garg T, Goyal AK. *Expert Opin. Drug Delivery.* 2014; 11:767.
- [99]. Dong CJ, Lv YG. *Polymers.* 2016; 8:20.
- [100]. Aamodt JM, Grainger DW. *Biomaterials.* 2016; 86:68. [PubMed: 26890039]
- [101]. Su K, Wang CM. *Biotechnol. Lett.* 2015; 37:2139. [PubMed: 26160110]
- [102]. Klotz BJ, Gawlitta D, Rosenberg A, Malda J, Melchels FPW. *Trends Biotechnol.* 2016; 34:394. [PubMed: 26867787]
- [103] a). de la Puente P, Ludena D. *Exp. Cell Res.* 2014; 322:1. [PubMed: 24378385] b) Shiu HT, Goss B, Lutton C, Crawford R, Xiao Y. *Tissue Eng. Part B-Rev.* 2014; 20:697. [PubMed: 24906469]
- [104]. Litvinov RI, Weisel JW. *Semin. Thromb. Hemost.* 2016; 42:333. [PubMed: 27056152]
- [105]. Hussein KH, Park KM, Kang KS, Woo HM. *Mater. Sci. Eng. C-Mater. Biol. Appl.* 2016; 67:766. [PubMed: 27287176]
- [106] a). Chen FM, Liu XH. *Prog. Polym. Sci.* 2016; 53:86. [PubMed: 27022202] b) Jang J, Kim TG, Kim BS, Kim SW, Kwon SM, Cho DW. *Acta Biomater.* 2016; 33:88. [PubMed: 26774760] c) Pati F, Ha DH, Jang J, Han HH, Rhie JW, Cho DW. *Biomaterials.* 2015; 62:164. [PubMed: 26056727]
- [107]. Swinehart IT, Badylak SF. *Dev. Dynamics.* 2016; 245:351.
- [108]. Higuchi A, Ling Q-D, Kumar SS, Chang Y, Alarfaj AA, Munusamy MA, Murugan K, Hsu S-T, Umezawa A. *J. Mater. Chem. B.* 2015; 3:8032.
- [109]. Visconti RP, Kasyanov V, Gentile C, Zhang J, Markwald RR, Mironov V. *Expert Opin. Biol. Ther.* 2010; 10:409. [PubMed: 20132061]
- [110]. Zhang YS, Yue K, Aleman J, Mollazadeh-Moghaddam K, Bakht SM, Yang J, Jia W, Dell'Erba V, Assawes P, Shin SR, Dokmeci MR, Oklu R, Khademhosseini A. *Ann. Biomed. Eng.* 2016; doi: 10.1007/s10439-016-1612-8
- [111]. Galie PA, Nguyen DH, Choi CK, Cohen DM, Janmey PA, Chen CS. *Proc. Natl. Acad. Sci. USA.* 2014; 111:7968. [PubMed: 24843171]
- [112]. Novosel EC, Kleinhans C, Kluger PJ. *Adv. Drug Delivery Rev.* 2011; 63:300.
- [113]. Jeyaraj R, G N, Kirby G, Rajadas J, Mosahebi A, Seifalian AM, Tan A. *Mater. Sci. Eng. C Mater. Biol. Appl.* 2015; 54:225. [PubMed: 26046286]

- [114]. Kinstlinger IS, Miller JS. *Lab Chip*. 2016; 16:2025. [PubMed: 27173478]
- [115]. Paulsen SJ, Miller JS. *Dev. Dyn*. 2015; 244:629. [PubMed: 25613150]
- [116]. Thottappillil N, Nair PD. *Vasc. Health Risk Manag*. 2015; 11:79. [PubMed: 25632236]
- [117] a). Huang AH, Niklason LE. *Cell. Mol. Life Sci*. 2014; 71:2103. [PubMed: 24399290] b) Mulligan-Kehoe MJ, Simons M. *Circulation*. 2014; 129:2557. [PubMed: 24934463]
- [118]. Nemen-Guanzon JG, Lee S, Berg JR, Jo YH, Yeo JE, Nam BM, Koh YG, Lee JI. *J. Biomed. Biotechnol*. 2012; 2012:956345. [PubMed: 23251085]
- [119]. Elliott MB, Gerecht S. *J. Mater. Chem. B*. 2016; 4:3443.
- [120] a). Briquez PS, Clegg LE, Martino MM, Gabhann FM, Hubbell JA. *Nat. Rev. Mater*. 2016; 1:15006. b) Egginton S. *Pflugers Arch*. 2009; 457:963. [PubMed: 18704490] c) Potente M, Gerhardt H, Carmeliet P. *Cell*. 2011; 146:873. [PubMed: 21925313]
- [121] a). Paulsen SJ, Miller JS. *Dev. Dyn*. 2015; 244:629. [PubMed: 25613150] b) Gui L, Niklason LE. *Curr. Opin. Chem. Eng*. 2014; 3:68. [PubMed: 24533306]
- [122]. Wu PK, Ringeisen BR. *Biofabrication*. 2010; 2:014111. [PubMed: 20811126]
- [123]. Seifu DG, Purnama A, Mequanint K, Mantovani D. *Nat. Rev. Cardiol*. 2013; 10:410. [PubMed: 23689702]
- [124]. Kolesky DB, Truby RL, Gladman AS, Busbee TA, Homan KA, Lewis JA. *Adv. Mater*. 2014; 26:3124. [PubMed: 24550124]
- [125]. Miller JS, Stevens KR, Yang MT, Baker BM, Nguyen DH, Cohen DM, Toro E, Chen AA, Galie PA, Yu X, Chaturvedi R, Bhatia SN, Chen CS. *Nat. Mater*. 2012; 11:768. [PubMed: 22751181]
- [126]. Kolesky DB, Homan KA, Skylar-Scott MA, Lewis JA. *Proc. Natl. Acad. Sci. USA*. 2016; 113:3179. [PubMed: 26951646]
- [127]. Lee VK, Kim DY, Ngo H, Lee Y, Seo L, Yoo SS, Vincent PA, Dai G. *Biomaterials*. 2014; 35:8092. [PubMed: 24965886]
- [128]. Lin H, Zhang D, Alexander PG, Yang G, Tan J, Cheng AW, Tuan RS. *Biomaterials*. 2013; 34:331. [PubMed: 23092861]
- [129]. Holmes B, Bulusu K, Plesniak M, Zhang LG. *Nanotechnology*. 2016; 27:064001. [PubMed: 26758780]
- [130]. Melchiorri AJ, Hibino N, Best CA, Yi T, Lee YU, Kraynak CA, Kimerer LK, Krieger A, Kim P, Breuer CK, Fisher JP. *Adv. Healthcare Mater*. 2016; 5:319.
- [131]. Zhang Y, Yu Y, Akkouch A, Dababneh A, Dolati F, Ozbolat IT. *Biomater. Sci*. 2015; 3:134. [PubMed: 25574378]
- [132]. Zhang Y, Yu Y, Ozbolat IT. *J. Nanotechnol. Eng. Med*. 2013; 4:020902.
- [133]. Luo Y, Lode A, Gelinsky M. *Adv. Healthcare Mater*. 2013; 2:777.
- [134]. Gao Q, He Y, Fu J.-z. Liu A, Ma L. *Biomaterials*. 2015; 61:203. [PubMed: 26004235]
- [135]. Xu C, Chai W, Huang Y, Markwald RR. *Biotechnol. Bioeng*. 2012; 109:3152. [PubMed: 22767299]
- [136]. Colosi C, Shin SR, Manoharan V, Massa S, Costantini M, Barbetta A, Dokmeci MR, Dentini M, Khademhosseini A. *Adv. Mater*. 2016; 28:677. [PubMed: 26606883]
- [137]. Jia W, Gungor-Ozkerim PS, Zhang YS, Yue K, Zhu K, Liu W, Pi Q, Byambaa B, Dokmeci MR, Shin SR, Khademhosseini A. *Biomaterials*. 2016; 106:58. [PubMed: 27552316]
- [138]. Bhattacharjee T, Zehnder SM, Rowe KG, Jain S, Nixon RM, Sawyer WG, Angelini TE. *Sci. Adv*. 2015; 1:e1500655. [PubMed: 26601274]
- [139]. Hinton TJ, Jallerat Q, Palchesko RN, Park JH, Grodzicki MS, Shue HJ, Ramadan MH, Hudson AR, Feinberg AW. *Sci. Adv*. 2015; 1:e1500758. [PubMed: 26601312]
- [140]. Meyer W, Engelhardt S, Novosel E, Elling B, Wegener M, Kruger H. *J. Funct. Biomater*. 2012; 3:257. [PubMed: 24955530]
- [141]. Stefan B, Franziska N, Ligon SC, Anneliese N, Helga B, David B, Jürgen S, Robert L. *Biomed. Mater*. 2011; 6:055003. [PubMed: 21849722]
- [142] a). Tan Y, Richards DJ, Trusk TC, Visconti RP, Yost MJ, Kindy MS, Drake CJ, Argraves WS, Markwald RR, Mei Y. *Biofabrication*. 2014; 6:024111. [PubMed: 24717646] b) Jakab K, Neagu

- A, Mironov V, Markwald RR, Forgacs G. Proc. Natl. Acad. Sci. USA. 2004; 101:2864. [PubMed: 14981244]
- [143]. Norotte C, Marga FS, Niklason LE, Forgacs G. Biomaterials. 2009; 30:5910. [PubMed: 19664819]
- [144]. Marga F, Jakab K, Khatiwala C, Shepherd B, Dorfman S, Hubbard B, Colbert S, Gabor F. Biofabrication. 2012; 4:022001. [PubMed: 22406433]
- [145]. Gu X. Front. Med. 2015; 9:401. [PubMed: 26482066]
- [146]. Jin X, Yamashita T. J. Biochem. 2016; 159:491. [PubMed: 26861995]
- [147]. Liu X, Pi B, Wang H, Wang X-M. Front. Mater. Sci. 2014; 9:1.
- [148]. Stichel CC, Muller HW. Prog. Neurobiol. 1998; 56:119. [PubMed: 9760698]
- [149]. Gu X, Ding F, Williams DF. Biomaterials. 2014; 35:6143. [PubMed: 24818883]
- [150]. Faroni A, Mobasser SA, Kingham PJ, Reid AJ. Adv. Drug Delivery Rev. 2015; 82–83:160.
- [151]. Belanger K, Dinis TM, Taourirt S, Vidal G, Kaplan DL, Egles C. Macromol. Biosci. 2016; 16:472. [PubMed: 26748820]
- [152]. Zhu W, O'Brien C, O'Brien JR, Zhang LG. Nanomedicine (Lond). 2014; 9:859. [PubMed: 24981651]
- [153]. Zhang, LG., Kaplan, DL. Neural Engineering: from Advanced Bio-materials to 3D Fabrication Techniques. Springer; Heidelberg: 2016.
- [154]. Saracino GA, Cigognini D, Silva D, Caprini A, Gelain F. Chem. Soc. Rev. 2013; 42:225. [PubMed: 22990473]
- [155]. Hsieh FY, Hsu SH. Organogenesis. 2015; 11:153. [PubMed: 26709633]
- [156]. Xu T, Gregory CA, Molnar P, Cui X, Jalota S, Bhaduri SB, Boland T. Biomaterials. 2006; 27:3580. [PubMed: 16516288]
- [157]. Ferris CJ, Gilmore KJ, Beirne S, McCallum D, Wallace GG, in het Panhuis M. Biomater. Sci. 2013; 1:224.
- [158]. Hopp B, Smausz T, Kresz N, Barna N, Bor Z, Kolozsvari L, Chrisey DB, Szabo A, Nogradi A. Tissue Eng. 2005; 11:1817. [PubMed: 16411827]
- [159]. Suri S, Han LH, Zhang W, Singh A, Chen S, Schmidt CE. Biomed. Microdevices. 2011; 13:983. [PubMed: 21773726]
- [160]. Curley JL, Jennings SR, Moore MJ. J. Vis. Exp. 2011; 48:e2636.
- [161]. Lee W, Pinckney J, Lee V, Lee JH, Fischer K, Polio S, Park JK, Yoo SS. Neuroreport. 2009; 20:798. [PubMed: 19369905]
- [162]. Pateman CJ, Harding AJ, Glen A, Taylor CS, Christmas CR, Robinson PP, Rimmer S, Boissonade FM, Claeysens F, Haycock JW. Biomaterials. 2015; 49:77. [PubMed: 25725557]
- [163]. Knowlton S, Cho Y, Li XJ, Khademhosseini A, Tasoglu S. Biomater. Sci. 2016; 4:768. [PubMed: 26890524]
- [164]. Luo C, Liu L, Ni X, Wang L, Nomura SM, Ouyang Q, Chen Y. Microelectron. Eng. 2011; 88:1707.
- [165]. Owens CM, Marga F, Forgacs G, Heesch CM. Biofabrication. 2013; 5:045007. [PubMed: 24192236]
- [166]. Hu Y, Wu Y, Gou Z, Tao J, Zhang J, Liu Q, Kang T, Jiang S, Huang S, He J, Chen S, Du Y, Gou M. Sci. Rep. 2016; 6:32184. [PubMed: 27572698]
- [167]. Jakus AE, Secor EB, Rutz AL, Jordan SW, Hersam MC, Shah RN. ACS Nano. 2015; 9:4636. [PubMed: 25858670]
- [168]. Lee YB, Polio S, Lee W, Dai G, Menon L, Carroll RS, Yoo SS. Exp. Neurol. 2010; 223:645. [PubMed: 20211178]
- [169]. Johnson BN, Lancaster KZ, Zhen G, He J, Gupta MK, Kong YL, Engel EA, Krick KD, Ju A, Meng F, Enquist LW, Jia X, McAlpine MC. Adv. Funct. Mater. 2015; 25:6205. [PubMed: 26924958]
- [170]. Lee S-J, Zhu W, Heyburn L, Nowicki M, Harris B, Zhang L. IEEE Trans. Biomed. Eng. 2016; : 99, 1.doi: 10.1109/TBME.2016.2558493 [PubMed: 27046866]

- [171]. Lorber B, Hsiao WK, Hutchings IM, Martin KR. *Biofabrication*. 2014; 6:015001. [PubMed: 24345926]
- [172]. Lozano R, Stevens L, Thompson BC, Gilmore KJ, Gorkin R 3rd, Stewart EM, in het Panhuis M, Romero-Ortega M, Wallace GG. *Biomaterials*. 2015; 67:264. [PubMed: 26231917]
- [173]. Hsieh FY, Lin HH, Hsu SH. *Biomaterials*. 2015; 71:48. [PubMed: 26318816]
- [174]. Gu Q, Tomaskovic-Crook E, Lozano R, Chen Y, Kapsa RM, Zhou Q, Wallace GG, Crook JM. *Adv. Healthcare Mater*. 2016; 5:1429.
- [175]. Radenkovic D, Solouk A, Seifalian A. *Med. Hypotheses*. 2016; 87:30. [PubMed: 26826637]
- [176]. Betts, JG. *Anatomy & Physiology*. Rice University; Houston: 2013.
- [177]. Duan B. *Ann. Biomed. Eng*. 2016; doi: 10.1007/s10439-016-1607-5
- [178]. Gaebel R, Ma N, Liu J, Guan J, Koch L, Klopsch C, Gruene M, Toelk A, Wang W, Mark P, Wang F, Chichkov B, Li W, Steinhoff G. *Biomaterials*. 2011; 32:9218. [PubMed: 21911255]
- [179]. Gaetani R, Doevendans PA, Metz CH, Alblas J, Messina E, Giacomello A, Sluijter JP. *Biomaterials*. 2012; 33:1782. [PubMed: 22136718]
- [180]. Hockaday LA, Kang KH, Colangelo NW, Cheung PY, Duan B, Malone E, Wu J, Girardi LN, Bonassar LJ, Lipson H, Chu CC, Butcher JT. *Biofabrication*. 2012; 4:035005. [PubMed: 22914604]
- [181]. Duan B, Kapetanovic E, Hockaday LA, Butcher JT. *Acta Biomater*. 2014; 10:1836. [PubMed: 24334142]
- [182]. Duan B, Hockaday LA, Kang KH, Butcher JT. *J. Biomed. Mater. Res. A*. 2013; 101:1255. [PubMed: 23015540]
- [183]. Ikegami T, Maehara Y. *Nat. Rev. Gastroenterol. Hepatol*. 2013; 10:697. [PubMed: 24126562]
- [184]. Wang X, Yan Y, Pan Y, Xiong Z, Liu H, Cheng J, Liu F, Lin F, Wu R, Zhang R, Lu Q. *Tissue Eng*. 2006; 12:83. [PubMed: 16499445]
- [185]. Chang R, Emami K, Wu H, Sun W. *Biofabrication*. 2010; 2:045004. [PubMed: 21079286]
- [186]. Nupura SB, Vijayan M, Solange M, Ali T, Masoumeh G, Mario M, Qi L, Yu Shrike Z, Su Ryon S, Giovanni C, Nasim A, Thomas DS, Colin EB, Anthony A, Mehmet RD, Ali K. *Biofabrication*. 2016; 8:014101. [PubMed: 26756674]
- [187]. Li S, Xiong Z, Wang X, Yan Y, Liu H, Zhang R. *J. Bioact. Compat. Polym*. 2009; 24:249.
- [188]. Robbins JB, Gorgen V, Min P, Shepherd BR, Presnell SC. *FASEB J*. 2013; 27:872.
- [189]. Nguyen D, Robbins J, Crogan-Grundy C, Gorgen V, Bangalore P, Perusse D, Creasey O, King S, Lin S, Khatiwala C, Halberstadt C, Presnell S. *FASEB J*. 2015; 29:LB424.
- [190]. Ma X, Qu X, Zhu W, Li YS, Yuan S, Zhang H, Liu J, Wang P, Lai CS, Zanella F, Feng GS, Sheikh F, Chien S, Chen S. *Proc. Natl. Acad. Sci. USA*. 2016; 113:2206. [PubMed: 26858399]
- [191]. Jung JW, Lee JS, Cho DW. *Sci. Rep*. 2016; 6:21685. [PubMed: 26899876]
- [192]. Do A-V, Akkouch A, Green B, Ozbolat I, Debabneh A, Geary S, Salem AK. *Ann. Biomed. Eng*. 2016; 1doi: 10.1007/s10439-016-1648-9
- [193]. Jonathan G, Karim A. *Int. J. Pharm*. 2016; 499:376. [PubMed: 26757150]
- [194]. Miao S, Zhu W, Castro NJ, Leng J, Zhang LG. *Tissue Engineering Part C: Methods*. 2016; 22:952. [PubMed: 28195832]
- [195] a). Peng W, Unutmaz D, Ozbolat IT. *Trends Biotechnol*. 2016; 34:722. [PubMed: 27296078] b) Zhu W, Castro NJ, Cui H, Zhou X, Boualam B, McGrane R, Glazer RI, Zhang LG. *Nanotechnology*. 2016; 27:315103. [PubMed: 27346678] c) Zhou X, Zhu W, Nowicki M, Miao S, Cui H, Holmes B, Glazer RI, Zhang LG. *ACS Appl. Mater. Interfaces*. 2016; 8:30017. [PubMed: 27766838]

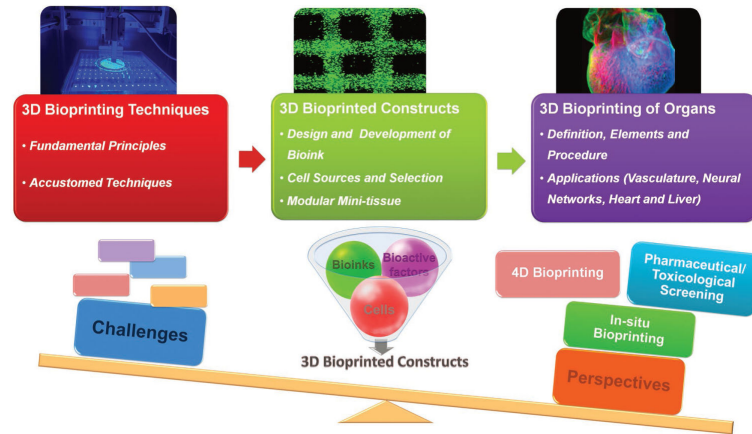


Figure 1. Schematic diagram outlining information covered in this review. Reproduced with permission.^[139] Copyright 2015, the American Association for the Advancement of Science.

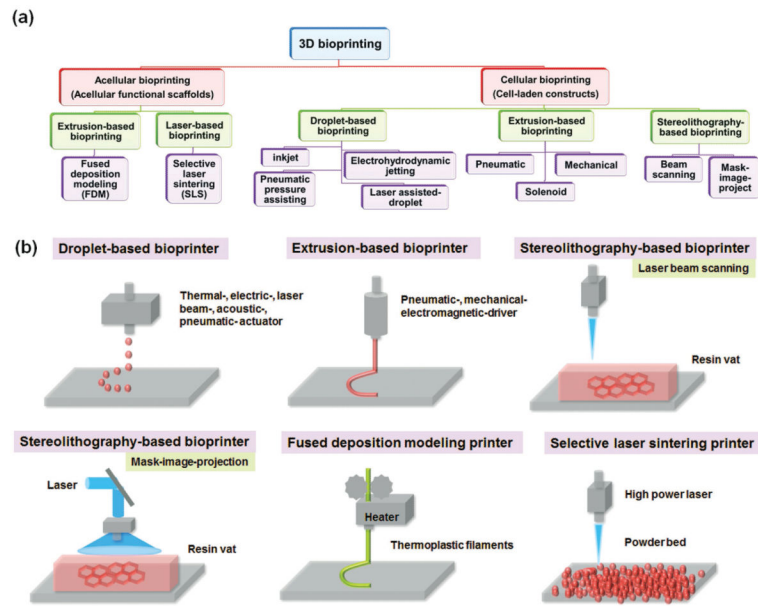


Figure 2. (a) A tree-diagram of the various 3D bioprinting techniques and (b) Simplified illustrations of typical 3D bioprinting techniques for tissue/organ regeneration.

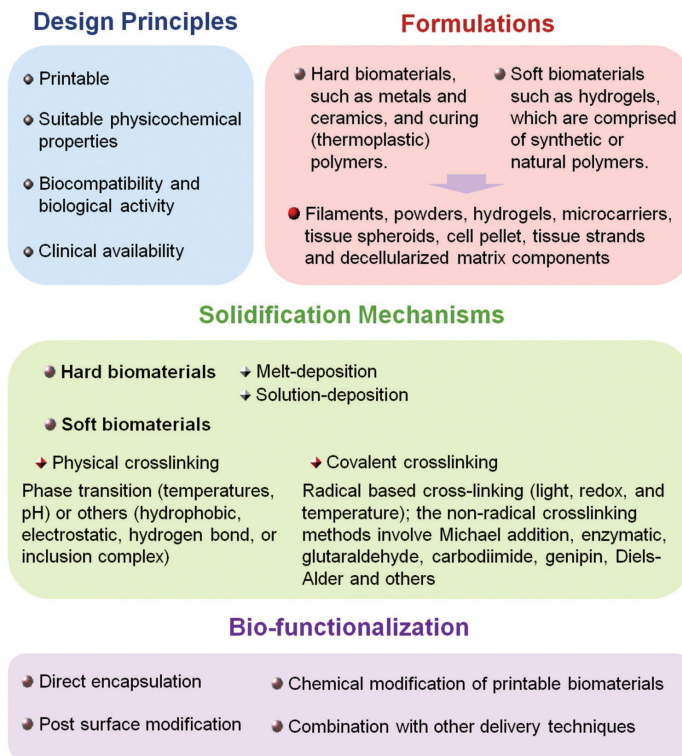


Figure 3. Design of bioinks for 3D bioprinting, including design principles, formulations, solidification mechanisms and bio-functionalization.

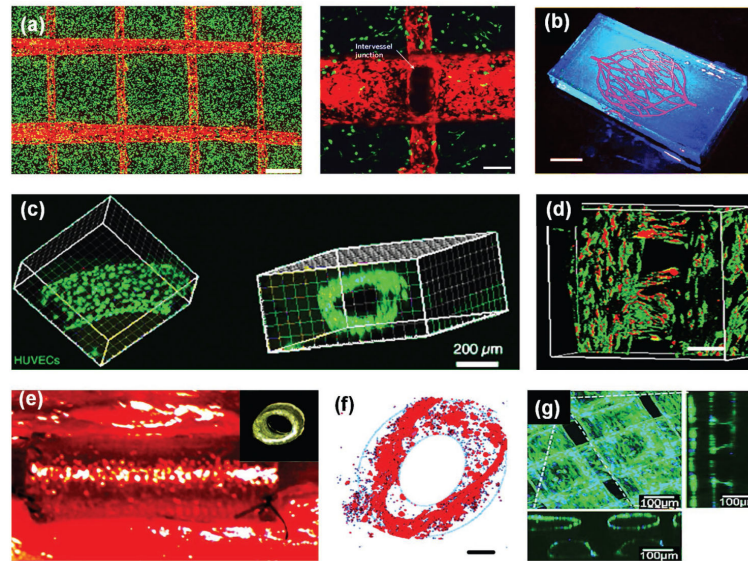


Figure 4.

(a) 3D printed perfusable vascularized tissue constructs. A confocal z-stack montage demonstrating HUVECs (expressing mCherry, red) were residing in the vascular space with 10T1/2 cells (expressing EGFP, green) uniformly distributed throughout a bulk fibrin gel, after one day in culture. Scale bar, 1 mm. A partial z-stack of two intersecting channels demonstrated endothelialization of channel walls and across the intervessel junction, while in the surrounding bulk gel 10T1/2 cells are seen beginning to spread out in three dimensions. Reproduced with permission.^[125] Copyright 2012, Nature Publishing Group.

(b) Fluorescent image of a 3D microvascular network fabricated via omnidirectional printing of a fugitive ink (dye red) within a photopolymerized Pluronic F127-diacrylate matrix. (Scale bar = 10 mm) Reproduced with permission.^[95] Copyright 2011, Wiley-VCH.

(c) Confocal image of live HUVEC cells lining the microchannel walls using the same fugitive ink method. Reproduced with permission.^[124] Copyright 2014, Wiley-VCH.

(d) Confocal fluorescence images of hMSCs and HUVECs co-cultured on various scaffolds in a static culture condition for 5 days. hMSCs were labeled with cell tracker green, and HUVECs were stained with cell tracker red. The scale bars indicate 200 μm . Reproduced with permission.^[85] Copyright 2016, Wiley-VCH.

(e) 3D-printed PPF scaffolds as venous interposition grafts at the time of in vivo implantation. Reproduced with permission.^[130] Copyright 2016, Wiley-VCH.

(f) Confocal fluorescence images of hMSCs and HUVECs co-cultured in designed vascular channel regions for 1 week. HUVECs encapsulated in the hydrogel were inclined to aggregate and migrate to form annular ring patterns along the channel. The scale bars indicate 200 μm . Reproduced with permission.^[87] Copyright 2016, Wiley-VCH.

(g) Confocal microscopy images show interconnected structures of the encapsulated HUVECs after migrating to outer regions of the bioprinted fibers at day 10. Reproduced with permission.^[136] Copyright 2015, Wiley-VCH.

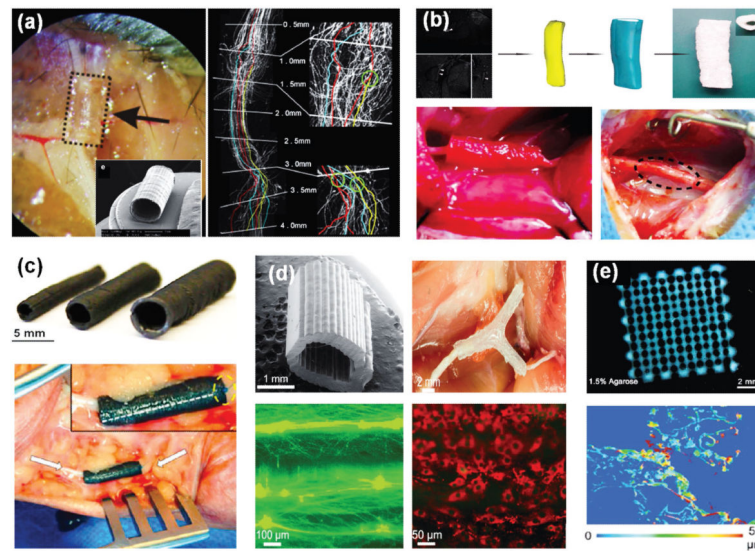


Figure 5.

(a) A PEG nerve guide made with a wall thickness of 50 μm by μSLA . The PEG nerve guide was implanted in to a Thy-1-YFP-H common fibular mouse, small gap, 3 mm injury model. The nerve graft repair image illustrated intervals marked with sample axon tracing from 4.0 mm interval position back to 0.0 mm (start) interval. The number of axons at each interval was counted to obtain a sprouting index value; axons were traced from distal intervals back to 0.0 mm, or a branch point with a previously traced axon (as highlighted in expanded sections with green circles), to calculate percentage of unique start axons represented at each interval. Reproduced with permission.^[162] Copyright 2015, Elsevier. (b) A patient's sciatic nerve was reconstructed based on MR neurography, and then a personalized nerve guidance conduit (NGC) was fabricated. The images show an intraoperative photograph of the NGCs for nerve regeneration in a rat sciatic nerve transection model with 10 mm gap, and the general observations of the regenerated sciatic nerve at 16 weeks post-surgery. Reproduced with permission.^[166] Copyright 2016, Nature Publishing Group. (c) 3D printed graphene nerve graft conduit at various sizes. Photograph of tubular nerve conduit that was implanted into a human cadaver via longitudinal transection and wrapped around the ulnar nerve (white arrows). The nerve conduit was then sutured closed along the previously described longitudinal transection (white dotted line) as well as to the surrounding epineurium and nerve tissue (inset, yellow circle). Excess 3DG nerve conduit length was then cut with surgical shears to expose additional nerve tissue. Reproduced with permission.^[167] Copyright 2015, American Chemical Society. (d) SEM image of a 3D printed hollow nerve pathway displaying an axially oriented physical cue on the luminal surface. Photograph of an implanted 3D printed nerve guide prior to suturing. Cultured primary embryonic neurons on the 3D printed, horizontally oriented physical cue (90° reference angle) stained for tau (green), while cultured Schwann cells on the horizontally oriented physical cue (90° reference angle) stained for GFAP (green) and laminin (red). Reproduced with permission.^[169] Copyright 2015, Wiley-VCH. (e) Printed gel scaffold comprising optimal 5% w/v alginate, 5% w/v carboxymethyl chitosan, and 1.5% w/v agarose. NSCs (31 d post-printing, including 21 d differentiation) stained with DAPI

(blue) and expressed TUJ1 (red), with cell clusters interconnected by neurites. The lower right panel shows depth coding of cells along the Z-axis (0–59 μm). Reproduced with permission.^[174] Copyright 2016, Wiley-VCH.

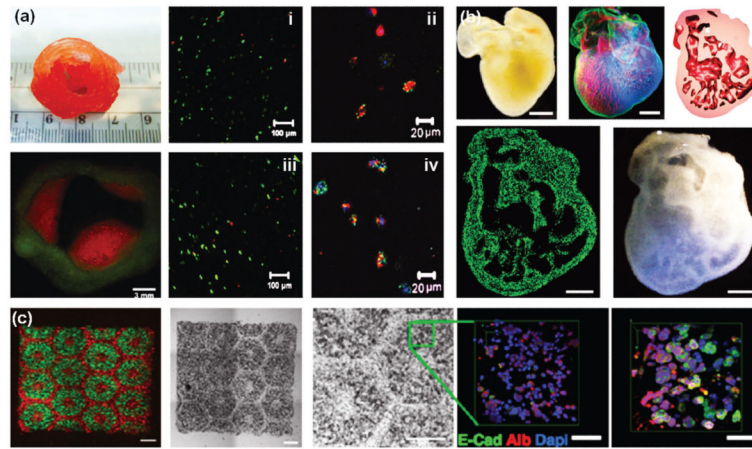


Figure 6.

(a) 3D printed aortic valve conduit. Fluorescent image of first two layers of a printed aortic valve conduit; SMC for valve root were labeled by cell tracker green and VIC for valve leaflet were labeled by cell tracker red. Live/dead assay for encapsulated VIC (i) in the leaflet and SMC (iii) in valve root after 7 day culture. Representative image of immunohistochemical staining for α SMA (green) and vimentin (red), and Draq 5 counterstaining for cell nuclei (blue); Staining for VIC (ii) in the leaflet, and staining for SMC (iv) in the root. Reproduced with permission.^[182] Copyright 2012, Wiley-VCH. (b) A dark field image of an explanted embryonic chick heart. A 3D image of the 5-day-old embryonic chick heart stained for fibronectin (green), nuclei (blue), and F-actin (red) and imaged with a confocal microscope. A cross section of the 3D CAD model of the embryonic heart with complex internal trabeculation based on the confocal imaging data. A cross section of the 3D printed heart in fluorescent alginate (green) showing recreation of the internal trabecular structure from the CAD model. A dark field image of the 3D printed heart with internal structure visible through the translucent heart wall via FRESH technique. Reproduced with permission.^[139] Copyright 2015, the American Association for the Advancement of Science. (c) Images (5 \times) taken under fluorescent and bright field channels showing patterns of fluorescently labeled hiPSC-HPCs (green) in 5% GelMA and supporting cells (red) in 2.5% GelMA with 1% GMHA on day 0. Scale bars, 500 μ m. Grayscale images (5 \times) and confocal immunofluorescence images (40 \times) showing albumin (Alb), E-cadherin (E-Cad), and nucleus (Dapi) staining of hiPSC-HPCs in 3D triculture constructs. Scale bars, 500 μ m in bright field and 100 μ m in fluorescent images. Reproduced with permission.^[190] Copyright 2016, National Academy of Sciences.